Invariance and stability conditions of interlayer synchronization manifold

Sarbendu Rakshit,[1] Bidesh K. Bera,[2,3] and Dibakar Ghosh[1,*]

[1]*Physics and Applied Mathematics Unit, Indian Statistical Institute, Kolkata 700108, India*

[2]*Department of Mathematics, Indian Institute of Technology Ropar, Punjab 140001, India*

[3]*Department of Solar Energy and Environmental Physics, BIDR, Ben-Gurion University of the Negev, Sede Boqer Campus, Midreshet Ben-Gurion, 8499000, Israel*

(Received 2 April 2019; revised manuscript received 2 January 2020; published 23 January 2020)

We investigate interlayer synchronization in a stochastic multiplex hypernetwork which is defined by the two types of connections, one is the intralayer connection in each layer with hypernetwork structure and the other is the interlayer connection between the layers. Here all types of interactions within and between the layers are allowed to vary with a certain rewiring probability. We address the question about the invariance and stability of the interlayer synchronization state in this stochastic multiplex hypernetwork. For the invariance of interlayer synchronization manifold, the adjacency matrices corresponding to each tier in each layer should be equal and the interlayer connection should be either bidirectional or the interlayer coupling function should vanish after achieving the interlayer synchronization state. We analytically derive a necessary-sufficient condition for local stability of the interlayer synchronization state using master stability function approach and a sufficient condition for global stability by constructing a suitable Lyapunov function. Moreover, we analytically derive that intralayer synchronization is unattainable for this network architecture due to stochastic interlayer connections. Remarkably, our derived invariance and stability conditions (both local and global) are valid for any rewiring probabilities, whereas most of the previous stability conditions are only based on a fast switching approximation.

DOI: 10.1103/PhysRevE.101.012308

I. INTRODUCTION

Complex network theory is one of the best platforms to understand several universal properties of a large number of interacting dynamical systems. Mathematically, a complex network is a pair $G = (X, E)$, where X and E denote the set of vertices and edges connecting the vertices, respectively. The studies on complex network theories gain immense attention for their wide range of applicability from the human brain to engineering systems to social sciences [1,2]. As many dynamical processes are best represented by network theory, so a study on combination of structural property and emerging collective behaviors has become an important research topic in numerous disciplines. For proper functioning, each node of the network is connected to the other nodes in various ways depending on the nature of interaction types.

Within a network, when a class of nodes interacts with other classes of nodes with more than one different way for their normal functioning, then such network is termed a *hypernetwork* [3,4]. In this type of network, the different types of connections are independent, which means that the existing link between any two nodes does not affect the other link between them. A hypernetwork is a pair $H = (X, E)$, where X is the set of nodes, $E = \{E^{[\alpha]} : \alpha = 1, 2, \ldots, M\}$ with $E^{[\alpha]} \subset X \times X$ is a nonempty set of edges and represents various interaction types in the tier α. Here M is the total number of tiers in the hypernetwork. Such types of interacting arrangements exist in many realistic networks. For instance, in the interneuronal communication network where two neurons connect through two structurally different types of synapses, one is electrical coupling via gap junction and another is the chemical synaptic function [5]. Other noticeable examples include the coordination behavior of the shoal of fish [6,7], where they use two types of cues to locate their mates: One is the visual perception cues and another is the secretion of the chemical signal. Also, in social systems, each individual person interacts with others at their workplace in some network architecture, and there may exist other independent network topologies corresponding to their family, friends, and many other social relations. Network of networks [8], power grid networks [9], computer communication networks [9], and many other realistic networks [10] are the best representation of the hypernetworks.

Another rapid growing research field is the study of synchronization in multilayered networks [11–13]. In multilayer network architecture, different classes of networks are organized within a single network, in which each set of nodes affects the other set of nodes. In general, such networks are composed of two or more different interacting layers and possess two types of interactions, namely intralayer and interlayer interactions. The former type of interaction refers to the coupling between the nodes within the same layer, whereas the second type corresponds to the interaction between the nodes in different layers. The mutual interaction types within the layer are not necessarily the same with the layer-layer interaction; they may be different. In graph-theoretical representation, a multilayer network with L number of layers is a pair $M = (G, C)$, where $G = \{G_\beta = (X_\beta, E_\beta) : \beta = 1, 2, \ldots, L\}$ is a family of

*dibakar@isical.ac.in

graphs each represents a layer. Here X_β and E_β are the set of edges and intralayer connections in the layer β, respectively. $C = \{E_{\beta_1\beta_2} \subset X_{\beta_1} \times X_{\beta_2} : \beta_1, \beta_2 \in \{1, 2, \ldots, L\}, \beta_1 \neq \beta_2\}$ is the set of interlayer connections between nodes of nonidentical layers. If in a multilayer network each layer has the same number of vertices and a given node only connected to its counterpart node in the rest of the layers, then it is known as a multiplex network. Therefore, for multiplex network, $|X_1| = |X_2| = ... = |X_L| = N$ and $E_{\beta_1\beta_2} = \{(v_i^{[\beta_1]}, v_i^{[\beta_2]}) : i = 1, 2, \ldots, N$ and $v_i^{[\beta_1]} \in X_{\beta_1}, v_i^{[\beta_2]} \in X_{\beta_2}\}$, where $|X|$ denotes the cardinality of the set X. The multilayered networks structure can capture the realistic description of the several real-world networks which include ecological networks [14], social networks [15], mobility networks [16], air-transportation networks [17], neuronal networks [18], etc. The global positioning system-continuously operating reference station (GPS-CORS) network is constructed of a physical layer and a data layer, which can also be regarded as a multilayer network [19]. Due to the presence of interconnections among the several complex systems [20,21], the multilayered network structure provides a good theory to better understand the various emerging phenomena such as percolation theory [9,22,23], epidemic spreading processes [24–27], controllability [28], diffusion processes [29] and congestion in traffic [30], evolutionary game dynamics [31], etc.

Among the several emerging behaviors in coupled systems, the synchronization phenomenon is one of the most interesting emerging subjects during the past few decades due to its enormous applicability in various fields of science [1,2]. This state refers to the adjustment of rhythms among the oscillators due to the interaction. Different types of synchronization properties were established theoretically and numerically in the multilayered formations, such as intra- and interlayer synchronizations [32–36], explosive synchronization [37], and cluster synchronization [38]. But in all of these cases, the underlying network topology is assumed to be time static, which means the interaction patterns are not changing over time. But in real-world situations, the interaction patterns are not always static in time; instead, they have temporal behavior in nature which means that the interaction links are always creating, destroying, or rewiring with different timescales [39]. For instance, there is the social interaction channel [40], where the social relationships among communities are incessantly changing over time. There are person-to-person communication networks [41], where the link between two individuals is not always active, but rather the edge is active only during their contact time. Also such time-varying features are often observed in various natural phenomena such as disease spreading [42], power transmission systems [43], process of chemotaxis [44], consensus problems [45], gene regulatory networks, protein-protein interactions [46], and functional brain networks [47]. In this context, since the late 2000s few studies have been done on synchronization in time-varying networks [4,48–52]. The emergence of synchronization in a multiplex dynamical network was studied in Ref. [53], where each layer is composed of mobile nodes performing in two-dimensional lattice random walk. However, the theory of interlayer synchronization (ILS) in time-varying multiplex hypernetwork is still in infancy. In this regard, here we address two questions: When will the ILS manifold be an invariant solution and What are the local and global stability conditions for the ILS state?

In this work, we investigate the ILS in a time-varying multiplex hypernetwork. In our case, each layer of the multiplex network possesses a hypernetwork architecture and all types of connections (intralayer as well as interlayer) are allowed to vary over time with characteristic rewiring probabilities. We propose a mathematical framework for invariance of the ILS state in a general stochastic multiplex hypernetwork. Then we analytically derive the necessary-sufficient condition for local stability of the ILS state through a master stability function approach [54]. We numerically validate our method by applying it to a multiplex network of Rössler oscillators with double interaction tiers in each layer. These two interaction tiers are associated with two structurally different coupling functions; one is through the x variable and another one through the y variable. The corresponding network architectures are assumed as Erdös-Rényi (ER) random network [55] and small-world (SW) network [56], respectively. Then we show that the Lyapunov spectra captures the stability of the ILS state in the time-varying networks. The obtained stability conditions for the ILS state are independent on the rewiring probabilities. We capture the ILS state in different parameter spaces and the results are agree well with the obtained linear stability analysis. By constructing a suitable Lyapunov function, the global stability condition for the ILS state is derived, which is also independent on rewiring probabilities. We also calculate the invariant condition for the emergence of the intralayer synchronization state. Due to the stochastic interlayer connections, the intralayer synchrony does not occur in our considered network architecture.

II. MATHEMATICAL MODEL OF STOCHASTIC MULTIPLEX HYPERNETWORK

A multilayer hypernetwork is an ordered pair $M_H = (G, C)$, where G is the collection of layers in which $E_\beta = \{E_\beta^{[\alpha]} : \alpha \in \{1, 2, \ldots, M\}\}$ is the family of hyperlinks for each tier α and C is the set of interlayer connections between nodes of nonidentical layers.

We consider a dynamical multiplex hypernetwork consisting of two layers, where each layer composed of more than one different types of interactions; each of these is called a *tier*. Here each of the two layers is composed of N number of nodes which are d-dimensional identical dynamical systems. In each layer, the nodes are interacting through M different tiers of connections, which represent different kinds of couplings among themselves. The states of the two layers are represented by the vectors $\mathbf{X} = \{\mathbf{x}_1, \mathbf{x}_2, \ldots, \mathbf{x}_N\}$ and $\mathbf{Y} = \{\mathbf{y}_1, \mathbf{y}_2, \ldots, \mathbf{y}_N\}$, where $\mathbf{x}_i, \mathbf{y}_i \in \mathbb{R}^d$. The mathematical form of the whole time-varying duplex hypernetwork is written as

$$\begin{aligned}
\dot{\mathbf{x}}_i &= F(\mathbf{x}_i) + \sum_{\alpha=1}^{M} \epsilon_\alpha \sum_{j=1}^{N} \mathscr{A}_{ij}^{[1,\alpha]}(t) G_\alpha(\mathbf{x}_i, \mathbf{x}_j) \\
&\quad + \eta\, b_i^{[1]}(t) H(\mathbf{x}_i, \mathbf{y}_i), \\
\dot{\mathbf{y}}_i &= F(\mathbf{y}_i) + \sum_{\alpha=1}^{M} \epsilon_\alpha \sum_{j=1}^{N} \mathscr{A}_{ij}^{[2,\alpha]}(t) G_\alpha(\mathbf{y}_i, \mathbf{y}_j) \\
&\quad + \eta\, b_i^{[2]}(t) H(\mathbf{y}_i, \mathbf{x}_i),
\end{aligned} \tag{1}$$

where i is the oscillator index ($i = 1, 2, \ldots, N$), N is the total number of oscillators in each layer, and the dynamics of each individual oscillator is governed by $F : \mathbb{R}^d \to \mathbb{R}^d$. Since our objective is to study the complete interlayer synchronization, so we consider identical vector field F. Here $H : \mathbb{R}^d \times \mathbb{R}^d \to \mathbb{R}^d$ represents the output vectorial function between the layers and $G_\alpha : \mathbb{R}^d \times \mathbb{R}^d \to \mathbb{R}^d$ is the output vectorial function within the layers corresponding to tier α. We assume that F is continuously differentiable with respect to its argument and all the coupling functions H and G_α are continuously differentiable with respect to both the arguments. Here ϵ_α is the intralayer coupling strength for the tier α which controls the interaction between the nodes in each layer. The interlayer coupling strength η determines how the information will be conveyed between the layers.

In the lth layer ($l = 1, 2$), the time-varying intralayer network configurations are encoded by the $N \times N$ adjacency matrices $\mathscr{A}^{[l,\alpha]}(t)$ which describe the interconnections between individual oscillators for the tier α. $\mathscr{A}^{[l,\alpha]}_{ij}(t) = 1$ if, in the layer l, the ith and jth nodes are connected through the tier α at time t and zero otherwise. Let $\mathscr{L}^{[l,\alpha]}(t)$ be the corresponding time-varying zero-row sum Laplacian matrix, where $\mathscr{L}^{[l,\alpha]}_{ij}(t) = -\mathscr{A}^{[l,\alpha]}_{ij}(t)$ if $i \neq j$ and $\mathscr{L}^{[l,\alpha]}_{ii}(t) = \sum_{j=1}^{N} \mathscr{A}^{[l,\alpha]}_{ij}(t)$. By rewiring each links stochastically and independently, the intralayer networks $A^{[l,\alpha]}(t)$ are varied over time with rewiring probability p_r. Specifically, at any time instant, we rewire each tier in the two layers independently by constructing a new network with probability p_r. Large p_r (i.e., $p_r \sim 1$) indicates very fast switching of the links, implying that the networks change rapidly, whereas $p_r \sim 0$ implies that the two layers are almost static as the links have a very low probability of change. Each of these successively created networks will be structurally equivalent due to the choice of fixed identical parameter values throughout the procedure. On the other hand, these two layers are connected by stochastic multiplexing over time. Here the interlayer connections are encrypted by the column matrices $b^{[1]}(t)$ and $b^{[2]}(t)$. $b^{[1]}_i(t) = 1$ [$b^{[2]}_i(t) = 1$] if there is a unidirectional connection from the ith node of the layer-2 (layer-1) to its counterpart node in the layer-1 (layer-2) at time t and zero otherwise. For a complete rigorous analysis, this is a sufficiently generalized model of speculative multiplex hypernetwork which allows enough connectionism for ILS state. With this general network architecture, we analyze the invariance and stability of the ILS state. Here our main emphasis is to study the ILS state by varying different coupling strengths and network parameters.

III. ANALYTICAL RESULTS

Interlayer synchronization is an emerging phenomenon of a multiplex network in which nodes of one layer evolve identically with its replica nodes of the different layers irrespective of whether the nodes in the same layer are in synchrony. Mathematically, network (1) is said to achieve complete ILS state if for all $i = 1, 2, \ldots, N$,

$$\|\mathbf{x}_i(t) - \mathbf{y}_i(t)\| \to 0 \text{ as } t \to \infty. \tag{2}$$

Then the ILS subspace can be defined as $\mathcal{S} = \{(\mathbf{x}_1(t), \mathbf{x}_2(t), \ldots, \mathbf{x}_N(t)) \subset \mathbb{R}^{dN} : \mathbf{x}_i(t) = \mathbf{y}_i(t), i = 1, 2, ..., N \text{ and } t \in \mathbb{R}^+\}$. This subspace is known as the ILS manifold. If this manifold is stable with respect to perturbations in the transverse subspace, then the interlayer synchronization can be observed physically. This type of state occurs when the individual oscillators of a multiplex network are appropriately coupled through intra- and interlayer coupling functions. In the next subsection, we investigate the invariance of the ILS manifold, i.e., What are the necessary conditions on the network architecture to emerge the interlayer synchrony?

A. Invariance of ILS manifold

A topological manifold which is invariant under the action of the dynamical system is known as an invariant manifold. The ILS manifold $\mathcal{S}$ is said to be an invariant solution of Eq. (1) if, starting from $\mathcal{S}$, the entire system still remains on $\mathcal{S}$ for all time t. In other words, if the replica-wise initial conditions are chosen identical, then the trajectories of each node will be identical with its counterpart node. Since our individual evolution function and all types of coupling functions (intra- and interlayer coupling functions) are identical for each node, we are interested to find the condition for the invariance of the manifold $\mathcal{S}$ in terms of the network architecture. In general, any multiplex hypernetwork architecture may not possess interlayer synchronization solution, unless the whole multiplex network is in global synchronization state. In this section, we are interested to find the invariant condition of the ILS state irrespective of synchrony in each layer.

To proof the ILS manifold is an invariant manifold, we have to show that if $\mathbf{x}_i(t_0) = \mathbf{y}_i(t_0)$, then $\mathbf{x}_i(t) = \mathbf{y}_i(t)$ for $t \geqslant t_0$. As we know that two dynamical systems starting with the same initial condition will evolve with the same trajectory if and only if their rate of changes are identical. Therefore, each replica starting from the same initial condition [$\mathbf{x}_i(t_0) = \mathbf{y}_i(t_0)$, $i = 1, 2, \ldots, N$] will remain in the same trajectory if and only if $\dot{\mathbf{x}}_i(t) = \dot{\mathbf{y}}_i(t)$, $i = 1, 2, \ldots, N$ for all $t \geqslant t_0$, which yields

$$\sum_{\alpha=1}^{M} \epsilon_\alpha \sum_{j=1}^{N} \big[\mathscr{A}^{[1,\alpha]}_{ij}(t) - \mathscr{A}^{[2,\alpha]}_{ij}(t)\big] G_\alpha(\mathbf{x}_i(t), \mathbf{x}_j(t)) + \eta\big[b^{[1]}_i(t) - b^{[2]}_i(t)\big] H(\mathbf{x}_i(t), \mathbf{x}_i(t)) = 0, \quad \forall\, t \geqslant t_0. \tag{3}$$

Now generally intralayer coupling functions and the underling connectivity networks are independent with that of interlayer. So the above equality will satisfy if and only if both the terms are independently zero, i.e.,

$$\sum_{\alpha=1}^{M} \epsilon_\alpha \sum_{j=1}^{N} \big[\mathscr{A}^{[1,\alpha]}_{ij}(t) - \mathscr{A}^{[2,\alpha]}_{ij}(t)\big] G_\alpha(\mathbf{x}_i(t), \mathbf{x}_j(t)) = 0 \tag{4}$$

and

$$\eta\big[b^{[1]}_i(t) - b^{[2]}_i(t)\big] H(\mathbf{x}_i(t), \mathbf{x}_i(t)) = 0, \tag{5}$$

for $t \geqslant t_0$ and $\alpha = 1, 2, \ldots, M$. Again the intralayer coupling functions corresponding to each tier are also independent due to different interaction mechanisms. Hence, for all time, their superposition can be zero only if the individual coefficients are zero. So Eq. (4) yields

$$\mathscr{A}^{[1,\alpha]}_{ij}(t) = \mathscr{A}^{[2,\alpha]}_{ij}(t), \tag{6}$$

for all $i, j \in \{1, 2, \ldots, N\}$ and $\alpha = 1, 2, \ldots, M$. The above relation implies that the adjacency matrices of the intralayer connections for both the layers should be same for each tier α.

From Eq. (5), we have

$$b_i^{[1]}(t) = b_i^{[2]}(t), \text{ or } H(\mathbf{x}_i(t), \mathbf{x}_i(t)) = 0, \tag{7}$$

for all $i = 1, 2, \ldots, N$. The above conditions indicate that the interlayer interaction should be either bidirectional or after achieving the interlayer synchronization corresponding coupling term should vanish, like diffusive coupling.

So the consequence is that, for the invariance of the ILS manifold of network Eq. (1), the necessary and sufficient conditions are

$$\mathscr{A}^{[1,\alpha]}(t) = \mathscr{A}^{[2,\alpha]}(t), \ t \in \mathbb{R}^+, \ \alpha = 1, 2, \ldots, M, \tag{8a}$$

$$b^{[1]}(t) = b^{[2]}(t), \ t \in \mathbb{R}^+, \text{ or } H(\mathbf{x}, \mathbf{x}) = 0. \tag{8b}$$

This invariant condition is valid for any rewiring probabilities of intra- and interlayer connections. Actually, for the time-varying networks, the invariant conditions of the synchronization state always being independent of the rewiring frequency. As time evolves, the underlying connections vary, but the topology will remain unchanged. For this reason, the rewiring frequency does not have any role in the existence of synchronization, but it plays a significant role in its stability due to the time-varying nature of the spectrum of the underlying networks. Hereafter, we will denote the common intralayer adjacency matrix corresponding to the tier α for both the layers by $\mathscr{A}^{[\alpha]}(t)$. Similarly, the column matrix $b(t)$ will denote the bidirectional interlayer connections, whenever it is.

This mathematical analysis captures the essential features of the stochastic multiplex hypernetwork to emerge the interlayer synchrony. This network may possess interlayer synchronization state by violating any one or both of these two conditions (8a) and (8b), but that will occur through global synchronization state [57]. Actually, for global synchronization state in the multilayer hypernetwork, all the nodes of the two layers evolve synchronously. That is, $\mathbf{x}_i(t) = \mathbf{x}_0(t)$ and $\mathbf{y}_i(t) = \mathbf{x}_0(t)$ for all $i = 1, 2, \ldots, N$, where $\mathbf{x}_0(t)$ is the global synchronization state of the entire network. In this situation, each replica is also in complete synchronization state, i.e., $\mathbf{x}_i(t) = \mathbf{y}_i(t)$ for all $i = 1, 2, \ldots, N$. Therefore, the complete synchronization state of the entire multilayer network implies the ILS state. While the invariant conditions (8a) and (8b) solely for ILS state not for global synchronization state. These conditions may be violated for the global synchronization induce ILS state. This type of ILS state through global synchrony is beyond the focus of the present study. It is to be noted that the simultaneous appearance of intralayer synchronization and ILS states in the multiplex network is triggered to the emergence of the global synchrony (the details proof given in Appendix A 1).

If the dynamical multiplex hypernetworks are solely in ILS state, not the intralayer synchronization state, then both invariant conditions (8a) and (8b) should be satisfied. To understand this in detail, let us first assume that system (1) is in interlayer synchronization, not in intralayer synchronization, and violating condition (8a).

Due to the interlayer coherence, we have $\mathbf{x}_i(t) = \mathbf{y}_i(t)$ for $i = 1, 2, \ldots, N$. Also, we have $\mathscr{A}^{[1,\alpha]}(t) \neq \mathscr{A}^{[2,\alpha]}(t)$ at least for one $\alpha \in \{1, 2, \ldots, M\}$. Then, for $i = 1, 2, \ldots, N$,

$$\dot{\mathbf{x}}_i(t) - \dot{\mathbf{y}}_i(t) = \sum_{\alpha=1}^{M} \epsilon_\alpha \sum_{j=1}^{N} \left[\mathscr{A}_{ij}^{[1,\alpha]}(t) - \mathscr{A}_{ij}^{[2,\alpha]}(t)\right] G_\alpha(\mathbf{x}_i, \mathbf{x}_j) \neq 0. \tag{9}$$

Although the state variables of the ith node are identical at time t, but their nonidentical velocity profiles cause the separation of their trajectories. Thus, if intralayer synchronization not occurs, then condition (8a) is the necessary and sufficient condition to induce the ILS state.

Again, if we assume that system (1) is in global synchronization with the identical intralayer structure and invariant condition (8b) is violated, then we have

$$\dot{\mathbf{x}}_i(t) - \dot{\mathbf{y}}_i(t) = \eta\left[b_i^{[1]}(t) - b_i^{[2]}(t)\right] H(\mathbf{x}_0, \mathbf{x}_0) \quad \neq 0. \tag{10}$$

Hence, even if the entire multiplex network is in a global synchronization state with identical intralayer structures, then the invariant condition (8b) should hold; otherwise, the ILS state is unattainable.

So, for invariance of the ILS state, we are assuming that the network typologies corresponding to the tier α are exactly identical in the two layers; in other words, their adjacency matrices are equal at each time instant. Then the dynamical evolution of the multiplex hypernetwork (1) becomes

$$\begin{aligned}
\dot{\mathbf{x}}_i &= F(\mathbf{x}_i) + \sum_{\alpha=1}^{M} \epsilon_\alpha \sum_{j=1}^{N} \mathscr{A}_{ij}^{[\alpha]}(t) G_\alpha(\mathbf{x}_i, \mathbf{x}_j) \\
&\quad + \eta\, b_i(t) H(\mathbf{x}_i, \mathbf{y}_i), \\
\dot{\mathbf{y}}_i &= F(\mathbf{y}_i) + \sum_{\alpha=1}^{M} \epsilon_\alpha \sum_{j=1}^{N} \mathscr{A}_{ij}^{[\alpha]}(t) G_\alpha(\mathbf{y}_i, \mathbf{y}_j) \\
&\quad + \eta\, b_i(t) H(\mathbf{y}_i, \mathbf{x}_i),
\end{aligned} \tag{11}$$

where $i = 1, 2, \ldots, N$. With the above structural viewpoint of invariance of the ILS state, Fig. 1 illustrates the interactions among nodes of such a temporal multiplex hypernetwork. For this schematic diagram, we consider $N = 10$ nodes and $M = 2$ different tiers of connections in each layer. The blue dashed and green solid lines represent the two interacting tiers. These two tiers are independent of each other; that is, the presence of a connection between two nodes in a tier does not influence the presence of connection in the other tiers. The hypernetworks in each layer comprised by these two coexisting tiers where each tiers have different kinds of links which represent different kind of interactions. Figures 1(a) and 1(b) respectively illustrate different interaction patterns for two different time instances, $t = t_1$ and $t = t_2$. For both the times, two tiers in each layer are exactly identical; moreover, the interlayer connections are varied stochastically.

Now we have derived the conditions for the existence of the ILS state for our considered time-varying multiplex hypernetwork [Eq. (1)]. In the next part, we derive the local and global stability conditions for ILS when the network [Eq. (1)] satisfies the invariant conditions (8a) and (8b). The local and global stability analyses for ILS state are done through

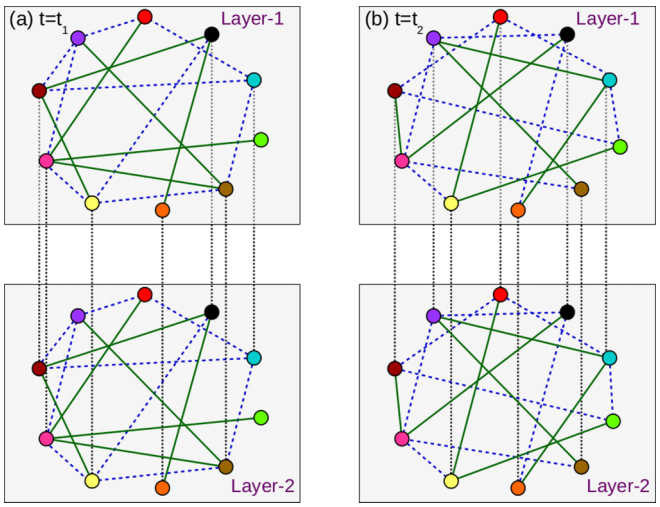

FIG. 1. Schematic of a multiplex hypernetwork consisting of two layers, each of size $N = 10$ for two different time instants: (a) $t = t_1$ and (b) $t = t_2$. Colored solid circles denote each individual nodes and black doted lines represent the interlayer connections. Each layer consists of two independent tiers, which are represented by blue dashed and green solid lines, and refer to different types of interaction modes. Identical color of a node and its replica node signifies the ILS state.

the master stability function approach and by constructing a suitable Lyapunov function, respectively.

B. Linear stability analysis

Now we derive the analytical stability condition for the ILS state in the coupled network [Eq. (11)] with bidirectional interlayer connections using the master stability function approach [54]. For a multiplex network of coupled Rössler oscillators, the master stability function also has been extended recently [57] by considering static intralayer and interlayer connections. In that paper [57], the analytical conditions for intralayer and interlayer synchronizations are discussed. If the ILS state occurs, then the ith replica evolves synchronously with the ILS manifold $\mathcal{S} = \{\mathbf{x}_i(t) = \mathbf{y}_i(t), i = 1, 2, \ldots, N\}$. This ILS state dominates the following evolution equations:

$$\dot{\mathbf{x}}_i = F(\mathbf{x}_i) + \sum_{\alpha=1}^{M} \epsilon_\alpha \sum_{j=1}^{N} \mathscr{A}_{ij}^{[\alpha]}(t) G_\alpha(\mathbf{x}_i, \mathbf{x}_j) + \eta\, b_i(t) H(\mathbf{x}_i, \mathbf{x}_i), \qquad i = 1, 2, \ldots, N. \tag{12}$$

Considering small perturbation $\delta\mathbf{z}_i(t)$ of the ith node of layer-2, its present state can be written as $\mathbf{y}_i(t) = \mathbf{x}_i(t) + \delta\mathbf{z}_i(t)$. Then linearizing this layer around the ILS state $\mathbf{x}_i(t)$, we obtain our required multiplex master stability equation transverse to the synchronization manifold as

$$\delta\dot{\mathbf{z}}_i = \{JF(\mathbf{x}_i) + \eta\, b_i(t)[JH(\mathbf{x}_i, \mathbf{x}_i) - DH(\mathbf{x}_i, \mathbf{x}_i)]\}\delta\mathbf{z}_i + \sum_{\alpha=1}^{M} \epsilon_\alpha \sum_{j=1}^{N} \mathscr{A}_{ij}^{[\alpha]}(t)[JG_\alpha(\mathbf{x}_i, \mathbf{x}_j)\delta\mathbf{z}_i + DG_\alpha(\mathbf{x}_i, \mathbf{x}_j)\delta\mathbf{z}_j], \tag{13}$$

for all $i = 1, 2, \ldots, N$. Here $JF(\mathbf{x}_i) = \frac{\partial F(\mathbf{x})}{\partial \mathbf{x}}|_{\mathbf{x}=\mathbf{x}_i}$, $JG_\alpha(\mathbf{x}_i, \mathbf{x}_j) = \frac{\partial G_\alpha(\mathbf{x},\mathbf{y})}{\partial \mathbf{x}}|_{(\mathbf{x},\mathbf{y})=(\mathbf{x}_i,\mathbf{x}_j)}$, $DG_\alpha(\mathbf{x}_i, \mathbf{x}_j) = \frac{\partial G_\alpha(\mathbf{x},\mathbf{y})}{\partial \mathbf{y}}|_{(\mathbf{x},\mathbf{y})=(\mathbf{x}_i,\mathbf{x}_j)}$, and $\mathbf{x}_i$ is the dynamics of the ILS state which satisfies Eq. (12). The similar derivation of the transverse master stability equation of the ILS state for static multilayer network can also be found in Ref. [58]. Now this master stability equation contains the time-varying intra- and interlayer connections. Additionally, its state variables evolve transverse to the ILS manifold, since all the error components are linearly independent. Therefore, the Lyapunov exponents of the above Eq. (13) are all transverse to the ILS manifold.

The above stability analysis for the ILS state is valid for any intra- and interlayer rewiring probabilities. As the rewiring probabilities change the intra- and interlayer connections, the Lyapunov exponent of the transverse error dynamics also vary accordingly. Analytically, it does not have any explicit dependence in the transverse error [Eq. (13)], but it comes through the connectivities matrices and numerically we observe the effect of rewiring probabilities (results are shown in Sec. IV B). Previous studies [4,35,59,60] on the stability of synchronization in time-varying networks are done for sufficiently high rewiring probability based on the fast switching approximation theory proposed in Ref. [61]. The obtained stability condition for the ILS state is irrespective of rewiring probability, whether it is slow or fast.

In some multiplex hypernetworks, the interlayer coupling function is unidirectional, e.g., neuronal hypernetwork where neurons communicate with each other through unidirectional chemical synapses [62]. The linear stability analysis for synchrony using unidirectional interlayer coupling functions is discussed in the Appendix A 2. In the next section, we validate our theoretical results by numerical illustrations.

IV. NUMERICAL ILLUSTRATIONS

In this section, our main emphasis is to identify the parameter regions for the ILS state, assessed by examining local asymptotic stability of the oscillators along synchronization manifold $\mathcal{S}$. In the time-varying network architecture [Eq. (11)], each node is associated with identical Rössler oscillator. We consider $N = 200$ number of oscillators and two structurally different interacting tiers in each layer. In the intralayer connection, two different types of interactions are considered here, which are associated with two structurally different coupling functions and network topologies. We take tier-1 as the ER random network with probability p_{rand} through the x variable and the corresponding network architecture is described by $\mathscr{L}^{[1]}(t)$. So each edge in the random graph is included with probability p_{rand} and independent from the other edges. In the another tier, each node is interacting through the y variable. The Laplacian matrix corresponding to this tier is $\mathscr{L}^{[2]}(t)$, which is considered the SW network constructed by the procedure proposed by Watts and Strogatz [56]. With regular ring coupling topology, we start with N nodes, where each node is connected with k nearest neighbors on each side. Then we reconnect all the initial edges with probability p_{sw} to the vertices chosen uniformly at random from distant nodes by avoiding dual edges. So the average degree of this SW network is $2k$. Then we rewire these two

intralayer networks with probability p_r. For the bidirectional random network, if there is an edge between the nodes i and j, then in the next iteration, the existing edge will be removed only if the network is rewired and then the edge between the ith and jth nodes will not be included. Therefore, for the random network, if there exists an edge between the nodes i and j, then in the next iteration that existing edge will be removed with probability $p_r(1 - p_{\text{rand}})$.

For the SW network, if two nearest neighbors are connected, then this existing connection will be removed only if the network is rewired and the nearest connection is replaced by a randomly chosen distant node. Therefore, if two nearest neighbors are connected, then with probability $p_r p_{\text{sw}}$, the existing connection will be replaced by a randomly chosen distant connection. Whereas $1 - p_{\text{sw}}$ is the probability of not reconnecting an initial edge to a distant node and leaving the edge as it is. Now, the connection between two distant neighbors is rewired with probability $p_r(1 - p_{sw})$ to the nearest neighbor node, if the network is rewired and then that nearest neighbor connection in the initial nonlocal ring keeps unchanged. However, each node in layer-1 is connected stochastically to its transcript node in layer-2 through the y variable with probability p_{inter}. The higher value of the $p_{\text{inter}}(\simeq 1)$ means that at every time step, almost every node is connected with its corresponding replica node, which makes the multilayer network a multiplex network. Similarly, $p_{\text{inter}} = 0$ denotes that the two layers are fully disconnected. To make stochastic interlayer connections, we choose p_{inter} from $(0, 1)$. In the prescribed dynamical multiplex hypernetwork [Eq. (11)], $F(\mathbf{x})$ denotes the individual dynamics of each oscillator, $H(\mathbf{x}_1, \mathbf{x}_2)$ represents the interlayer coupling function, and intralayer coupling functions are denoted by $G_1(\mathbf{x}_1, \mathbf{x}_2)$, $G_2(\mathbf{x}_1, \mathbf{x}_2)$ and are given by the following mathematical forms:

$$F(\mathbf{x}) = \begin{bmatrix} -y - z \\ x + ay \\ b + z(x - c) \end{bmatrix}, \quad H(\mathbf{x}_1, \mathbf{x}_2) = \begin{pmatrix} 0 \\ y_1 - y_2 \\ 0 \end{pmatrix},$$

$$G_1(\mathbf{x}_1, \mathbf{x}_2) = \begin{pmatrix} x_1 - x_2 \\ 0 \\ 0 \end{pmatrix}, \quad G_2(\mathbf{x}_1, \mathbf{x}_2) = \begin{pmatrix} 0 \\ y_1 - y_2 \\ 0 \end{pmatrix}.$$

We fix the parameters at $a = 0.2$, $b = 0.2$, and $c = 5.7$, for which all the trajectories of the Rössler system eventually enter into a compact set which accumulates in the neighborhood of a chaotic attractor. We numerically integrate the entire network using a fourth-order Runge-Kutta method with integration time step $dt = 0.01$ by taking fixed initial conditions from the phase space volume $[-0.01, 0.01] \times [-0.01, 0.01] \times [0, 0.01]$. This fixed initial condition is chosen randomly from the phase-space volume. To draw the numerical figures, we have taken 20 network realizations at each point. For numerical simulation, we have rewired the edges with respective probabilities at each integration time step.

For multiplex network, the ILS occurs when each subsystem in a given layer evolves synchronously with its counterpart node in the other layer. Here we delve into the ILS state of the temporal multiplex hypernetwork by changing the coupling strengths and network parameters. To measure the ILS state, the following error is introduced:

$$E = \lim_{T\to\infty} \frac{1}{T} \int_0^T \sum_{i=1}^{N} \frac{\|\mathbf{x}_i(t) - \mathbf{y}_i(t)\|}{N} dt, \tag{14}$$

where $\|\cdot\|$ is the Euclidean norm operator and T is a large positive real number. To measure E, the time interval is taken over 1×10^5 units after an initial transient of 2×10^5 units. In simulation, we have used the threshold value for the interlayer synchronization error as 10^{-5}.

By associating the paradigmatic Rössler oscillator in each node, our required equation of motion of the transverse error systems becomes

$$\begin{aligned} \dot{\xi}_i^{(x)} &= -\xi_i^{(y)} - \xi_i^{(z)} - \epsilon_1 \sum_{j=1}^{N} \mathscr{L}_{ij}^{[1]}(t)\xi_j^{(x)}, \\ \dot{\xi}_i^{(y)} &= \xi_i^{(x)} + a\xi_i^{(y)} - \epsilon_2 \sum_{j=1}^{N} \mathscr{L}_{ij}^{[2]}(t)\xi_j^{(y)} - 2\eta b_i(t)\xi_i^{(y)}, \\ \dot{\xi}_i^{(z)} &= z_i\xi_i^{(x)} + (x_i - c)\xi_i^{(z)}, \end{aligned} \tag{15}$$

where the evolution equation of the ILS manifold is

$$\begin{aligned} \dot{x}_i &= -y_i - z_i - \epsilon_1 \sum_{j=1}^{N} \mathscr{L}_{ij}^{[1]}(t)x_j, \\ \dot{y}_i &= x_i + ay_i - \epsilon_2 \sum_{j=1}^{N} \mathscr{L}_{ij}^{[2]}(t)y_j, \\ \dot{z}_i &= b + z_i(x_i - c), \quad i = 1, 2, \ldots, N. \end{aligned} \tag{16}$$

The exponential expansion or contraction rate of an infinitesimal perturbations can be measured by Lyapunov exponents. This can be ascertained by the linearized Eq. (15) with respect to the reference trajectory satisfying Eq. (16). Among all the Lyapunov exponents Λ_j, $j = 1, 2, \ldots, dN$ of Eq. (15), the largest one will be called the maximum Lyapunov exponent (MLE) and denoted by Λ. It plays a key roll for stability of the ILS state. For the desynchronized state, where the individual oscillators are chaotic, the error state variable $\xi(t)$ evolves chaotically. So for that case, Λ will be greater than zero. By adjusting the coupling strength if the ILS state occurs, then $\xi \to 0$ as $t \to \infty$. Due to the stabilization of system (15) at that coupling strength, Λ becomes negative. The maximum of the Lyapunov exponent as a function of the parameters $(\epsilon_1, \epsilon_2, \eta)$ gives the necessary condition for the local stability of the ILS state. Whenever $\Lambda < 0$, the perturbations transverse to that manifold die out, and all the replicas evolve in unison. So the negativity of Λ obtain from the linearized Eq. (15) together with ILS manifold Eq. (16) implies the stable ILS state.

In the following parts, we explore the effect of two different intralayer coupling strengths ϵ_1 and ϵ_2 corresponding to the ER and SW networks, respectively, on the emergence of the ILS state. The parameter η represents the interlayer coupling strength and we fix $\eta = 1.0$. We also explore the influence of other network parameters, namely p_{inter} (interlayer connection probability), p_r (intralayer rewiring probability), p_{rand} (ER

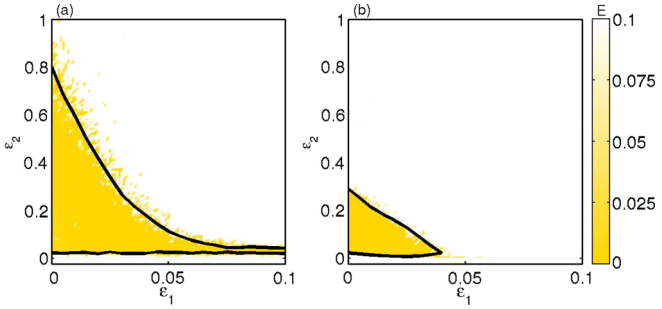

FIG. 2. Effect of intralayer coupling values ϵ_1 and ϵ_2 on the transition of interlayer synchronization characterize through the interlayer synchronization error E for (a) $p_r = 10^{-6}$ and (b) $p_r = 0.01$. The black lines denote the critical curves for $\Lambda = 0$. Yellow and white portions represent the region of stable and unstable ILS state, respectively. Other parameters are fixed at $p_{\text{sw}} = 0.1$, $p_{\text{rand}} = 0.015$, $p_{\text{inter}} = 0.05$, and $k = 2$.

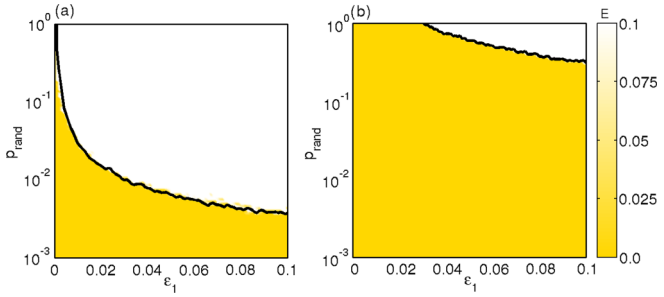

FIG. 3. Variation of interlayer synchronization error in (ϵ_1, p_{rand}) plane for (a) $p_{\text{inter}} = 0.05$ and (b) $p_{\text{inter}} = 0.1$ with fixed other parameter values at $p_{\text{sw}} = 0.1$, $p_r = 0.001$, $\epsilon_2 = 0.2$, and $k = 2$. The black line represents the critical curve for which $\Lambda = 0.0$; above and below this curve denotes the regions for $\Lambda > 0.0$ (unstable ILS state) and $\Lambda < 0.0$ (stable ILS state), respectively.

network probability), and p_{sw} (small-world probability) for the emergence of interlayer synchrony. Now we start our investigations with the numerical results and simultaneously we validate these results with the help of analytical findings. In the next two subsections, we will explore the effect of the coupling strengths and the rewiring probabilities one by one.

A. Effect of coupling strengths

Now we investigate the effect of the intralayer coupling strengths ϵ_1 and ϵ_2 on the ILS state. For the network consisting of one layer and one tier, the effect on coupling strengths for various inner coupling matrices has been discussed in Ref. [63] by taking several paradigmatic models. Here we have opted for the interlayer coupling through the y variable. In the network of Rössler oscillators with this type of coupling, if synchronization occurs once, then it persists for further higher coupling strengths. Therefore, in the absence of all intralayer couplings, Λ has only one cross point along the η axis, and it remains negative in the large-η limit. While in the absence of interlayer coupling strength (i.e., $\eta = 0$), the synchrony in a single layer with hypernetwork architecture enhances the parameter region in (ϵ_1, ϵ_2) plane (results not shown here). For one tier in this single-layer network, the critical values of coupling strength are (i) $\epsilon_1^* = [0.07, 0.2]$, when $\epsilon_2 = 0.0$ and (ii) $\epsilon_2^* = [1.5, \infty)$, when $\epsilon_1 = 0.0$, where the other parameter values are fixed at $p_r = 10^{-6}$, $p_{\text{sw}} = 0.1$, $k = 2$, and $p_{\text{rand}} = 0.05$. Interestingly, highly rich complex behavior arises when we consider the stochastic multiplex configuration with $\eta \neq 0.0$. In the next two parts, we discuss the effect of different parameters on the ILS state and demonstrate the results systematically.

First, we are interested to see the simultaneous effect of the intralayer coupling strengths ϵ_1 and ϵ_2 corresponding to the hypernetwork organizations. We obtain the synchronization region in (ϵ_1, ϵ_2) parameter space in Fig. 2 by taking two different intralayer rewiring probabilities. Here all the other parameters are fixed at $p_{\text{sw}} = 0.1$, $p_{\text{rand}} = 0.015$, $p_{\text{inter}} = 0.05$, and $k = 2$. Figure 2(a) is plotted for $p_r = 10^{-6}$, that is, when the intralayer networks are almost static. Here we observe that when $\epsilon_1 = 0.0$, the critical value of ϵ_2 for the emergence of interlayer synchrony is 0.02 and this synchrony persists up to $\epsilon_2 = 0.8$. Whereas, in the absence of intralayer coupling in the y variable (i.e., $\epsilon_2 = 0.0$), coupling through the x variable is unable to emerge synchronously. But when increasing values of ϵ_1, this synchrony region gradually decreases. Finally, for $\epsilon_1 = 0.1$, the synchrony region is confined within $\epsilon_2 \in [0.02, 0.04]$. For higher value of ϵ_1, the ILS does not emerge for any values of ϵ_2. This type of result can be seen if we increase the rewiring probability $p_r = 0.01$ in Fig. 2(b) and the synchronization emerges within $\epsilon_2 \in [0.02, 0.28]$ for $\epsilon_1 = 0.0$. Also as we increase ϵ_1, this region gradually shrinks and finally the synchrony region vanishes at $\epsilon_1 = 0.039$. Therefore, the higher rewiring probabilities give rise to the narrow synchronization regions. Here the interesting thing is that the ILS region is suppressed for sufficient rapid switching of the intralayer links. It is physically reasonable that when nodes are more involved within the layer interactions compare to their replica layer then it is obvious to loss their interlayer rhythmic adjustment which are reflected in this picture (Fig. 2). Also, it gives us a clue as to how to control the ILS without effecting the interlayer connection.

Now we verify the numerically obtained ILS region (yellow regions in Fig. 2) in the (ϵ_1, ϵ_2) parameter plane by the maximum transverse Lyapunov exponent Λ which is calculated from Eq. (15) along with Eq. (16). The critical curves of the ILS state characterized by the MLE (i.e., when $\Lambda = 0$) are shown as black lines in Figs. 2(a) and 2(b). In the yellow regions, the value of $\Lambda < 0$ signifies the stable ILS state and $\Lambda > 0$ in the white region (unstable ILS state).

Next, we investigate the emergence of interlayer synchrony under the simultaneous influences of random network probability p_{rand} (a intralayer network parameter) and corresponding intracoupling value ϵ_1. With the interplay of these two parameters, we explore the occurrence of ILS in $(\epsilon_1, p_{\text{rand}})$ plane for two different values of the interlayer rewiring probabilities $p_{\text{inter}} = 0.05$ and $p_{\text{inter}} = 0.1$. The results are shown in Figs. 3(a) and 3(b), respectively. In Fig. 3(a), one can see that for $\epsilon_1 = 0.0$, the systems are in the ILS state. But when we slight increase the values of ϵ_1, a desynchrony region appears even for higher values of p_{rand}. For further increasing values of ϵ_1, the synchrony region monotonically shrinks. Finally, at $\epsilon_1 = 0.1$, the interlayer synchrony persists

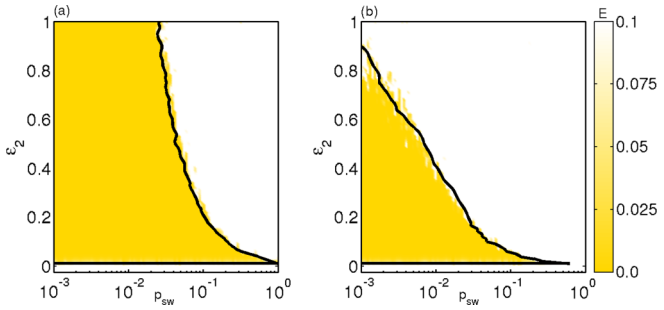

FIG. 4. Dependency of interlayer synchronization on the mean degrees in the parameter plane of p_{sw} and ϵ_2 for (a) $k = 2$ and (b) $k = 5$. The black line represents the critical curve where $\Lambda = 0.0$. Other parameter values are $p_{rand} = 0.015$, $p_r = 0.001$, $p_{inter} = 0.06$, and $\epsilon_1 = 0.025$.

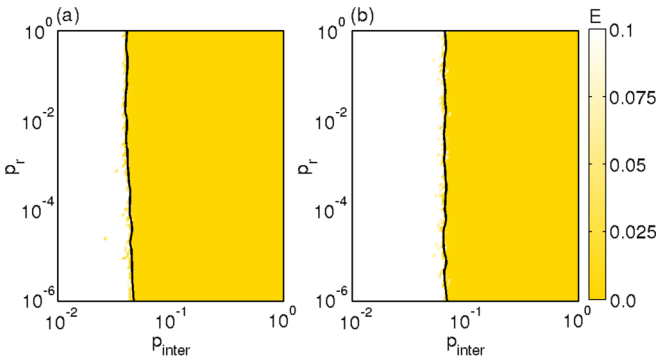

FIG. 5. Variation of the interlayer synchronization error with respect to p_{inter} and p_r for (a) $\epsilon_1 = 0.01$, $\epsilon_2 = 0.1$ and (b) $\epsilon_1 = 0.07$, $\epsilon_2 = 0.7$. Other parameter values are $p_{sw} = 0.1$, $k = 2$ and $p_{rand} = 0.015$. Black curves represent the critical curve for which $\Lambda = 0$.

up to $p_{rand} = 0.003715$. So when the underlying network approaches the global network form sparse network, the synchrony state slowly ruptured. For higher values of $p_{inter} = 0.1$, no desynchronization region comes into the picture up to $\epsilon_1 = 0.03$ [Fig. 3(b)]. After $\epsilon_1 = 0.03$, the ILS state becomes unstable for large values of p_{rand}. But for further increasing values of ϵ_1, this critical value of p_{rand} for ILS gradually decreases. Finally, at $\epsilon_1 = 0.1$, the interlayer synchrony persists up to $p_{rand} = 0.309$. From this result, we can conclude that the probability of the underlying random network and the coupling on the x variable are both unfavorable for the interlayer synchrony. More importantly, it is observed that the ILS region in the (ϵ_1, p_{rand}) plane enhances only for sufficient fast switching of interlayer links between the layers.

We evaluate the maximum transverse Lyapunov exponent Λ with respect to the probability of the random network p_{rand} and x variable intralayer coupling strength ϵ_1. The critical curves of synchrony are shown as a black line in Figs. 3(a) and 3(b) for $p_{inter} = 0.05$ and $p_{inter} = 0.1$, respectively. For both the panels when the probability of the random network is very low it remains in the ILS state; however, for higher values, the synchrony breaks. In the left panel for $\epsilon_1 = 0.01$, first desynchrony occurs at $p_{rand} = 0.03981$, and for $\epsilon_1 = 0.03$, this transition happens at $p_{rand} = 0.014$. Further increasing the values of $\epsilon_1 = 0.05$, it occurs at $p_{rand} = 0.007$, and for $\epsilon_1 = 0.07$ and $\epsilon_1 = 0.09$, the critical values of p_{rand} are respectively 0.0055 and 0.005. In the right panel for $p_{inter} = 0.1$, a similar shrinking tendency is observed but the transition region is shifted toward the right. For $\epsilon_1 = 0.035$, a desynchrony region occurs at the critical value $p_{rand} = 0.7$. By increasing the values of ϵ_1, this critical value monotonically decreases; finally, at $\epsilon_1 = 0.1$, the exchange of the stability of the ILS state happens at $p_{rand} = 0.25$.

Now we explore the influence of SW probability p_{sw} and the corresponding y-variable coupling strength ϵ_2 on the ILS state. The value of p_{sw} near zero represents the regular network topology, whereas closer to 1 it represents the random network, and it denotes the SW topology for certain intermediate values of p_{sw}. In Fig. 4 the color bar shows the continuous variation of the synchronized error by simultaneously changing of p_{sw} and ϵ_2 for two different mean degrees k. For all the values of average degree of the SW network, the interlayer coherence can occurs only after $\epsilon_2 =$ 0.02 irrespective of the values of p_{sw}. Figure 4(a) is plotted for average degree of SW network $k = 2$. Before $p_{sw} = 0.024$, no desynchronization region emerges in this figure; however, at $p_{sw} = 0.024$, the desynchronization region appears at $\epsilon_2 = 1.0$. For further higher values of p_{sw}, the critical coupling strength of ϵ_2 for the appearance of the desynchrony gradually decreases. After $p_{sw} = 0.2188$, no interlayer synchronization region is seen for all values of ϵ_2 in [0,1]. For a SW network with higher average degree, $k = 5$, the shrinking of the synchronization region in the (p_{sw}, ϵ_2) plane is depicted in Fig. 4(b). Here for $p_{sw} = 10^{-3}$, one can get the synchronization region within $\epsilon_2 \in [0.02, 0.7]$. However for higher values of p_{sw}, this synchronization region monotonically decreases, and, finally, it annihilates at $p_{sw} = 0.06761$. So the higher mean degree k of the SW network destroys the interlayer coherence in the SW probability p_{sw} and the y-variable coupling strength ϵ_2 parameter space. The stability curves of the interlayer synchrony is also verified by calculating the value of Λ in the parameter space (p_{sw}, ϵ_2) for $k = 2$ and $k = 5$ in Figs. 4(a) and 4(b), respectively. The region between these two black curves is the region of synchrony, which is an excellent agreement with the numerical simulations.

B. Effect of rewiring probabilities

Now we investigate the role of interlayer and intralayer rewiring probabilities p_{inter} and p_r on the emergence of the ILS state. For this, we study the effect of p_{inter} by simultaneous changes of p_r and ϵ_2. The synchronization and desynchronization regions are plotted in the (p_{inter}, p_r) plane by taking two sets of intralayer coupling strengths: $\epsilon_1 = 0.01$, $\epsilon_2 = 0.1$ [for Fig. 5(a)] and $\epsilon_1 = 0.07$, $\epsilon_2 = 0.7$ [for Fig. 5(b)]. The color bar shows the variation of ILS error E. The probability of the random network is fixed at $p_{rand} = 0.015$, SW probability $p_{sw} = 0.1$, with the average degree of the SW network at $k = 2$. For lower intralayer strengths $\epsilon_1 = 0.01$ and $\epsilon_2 = 0.1$, slight enhancement of the ILS state is observed in Fig. 5(a). For very small values of $p_r = 10^{-6}$, the critical value of p_{inter} is 0.04786. However, for higher values of intralayer rewiring probability $p_r = 10^0$, this critical value enhances to $p_{inter} = 0.04365$. When the intralayer coupling strengths

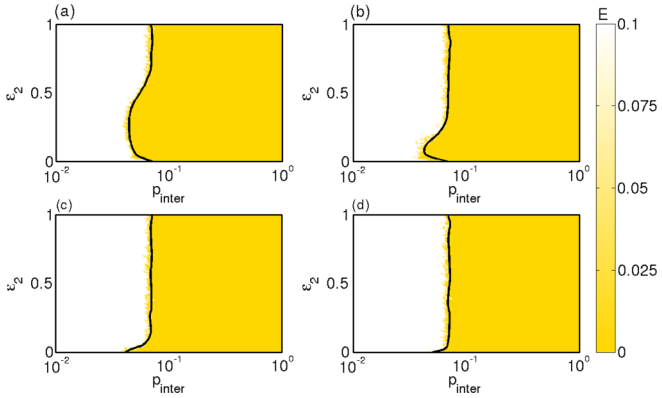

FIG. 6. Transition of interlayer synchrony in the $(p_{\text{inter}}, \epsilon_2)$ plane for (a) $\epsilon_1 = 0.0$, (b) $\epsilon_1 = 0.025$, (c) $\epsilon_1 = 0.05$, and (d) $\epsilon_1 = 0.075$. Other parameters: $p_{\text{sw}} = 0.1$, $p_{\text{rand}} = 0.015$, $p_r = 0.001$, and $k = 2$. The black lines represent the critical curves for which $\Lambda = 0.0$; the curves to the left and right denote the regions for $\Lambda > 0.0$ (unstable ILS state) and $\Lambda < 0.0$ (stable ILS state), respectively.

are increased at $\epsilon_1 = 0.07$, $\epsilon_2 = 0.7$, this tiny enhancement vanishes [Fig. 5(b)] and the intralayer rewiring probability has no influence on the appearance of interlayer synchrony. Here the critical value of p_{inter} is same for almost all values of p_r, which is 0.07244. The critical curves of synchrony, that is, when $\Lambda = 0$, are shown as black lines in Figs. 5(a) and 5(b). So for sufficient higher intralayer interaction strengths, the intralayer rewiring probability does not have any effect on the ILS state and is fully determined by the critical value of p_{inter}.

Finally, we explore the effect of ILS regions by simultaneously varying p_{inter} and ϵ_2 for different values of ϵ_1. Here we want to see how the intralayer coupling strengths are related to the p_{inter} on the occurrence of the ILS state with fixed other network parameters associated with intralayer connections. The desynchronized and synchronized regions are characterized through the synchronization error E whose variations are shown in the color bar. Figure 6(a) is plotted for $\epsilon_1 = 0.0$, i.e., in absence of the x coupling. Interestingly, in this parameter plane, a mixed type of synchronization transition is observed. Here ILS enhances up to $\epsilon_2 = 0.25$, and beyond that the coupling strength, i.e., de-enhancement of the ILS state, occurs for higher values of ϵ_2. After certain values of $\epsilon_2 = 0.6$, interlayer interaction probability does not have any effect on ϵ_2 and becomes fully discerned on the values of p_{inter}. In Fig. 6(b), the region of this mixed type of behavior contracted for $\epsilon_1 = 0.025$. Here the enhancement of the ILS state occurs up to $\epsilon_2 = 0.05$, and beyond that the de-enhancement happens up to $\epsilon_2 = 0.25$. Ultimately, the synchrony pattern becomes independent of ϵ_2. With further higher values of ϵ_2, ILS occurs after the critical values of $p_{\text{inter}} = 0.07586$. In Fig. 6(c) for $\epsilon_1 = 0.05$, the small enhancement–de-enhancement region is bounded within $\epsilon_2 = 0.1$, and after that synchrony emerges for all $p_{\text{inter}} \geqslant 0.07586$. For $\epsilon_1 = 0.075$ in Fig. 6(d), the mixed region almost vanishes and the ILS state occurs only after certain critical values of $p_{\text{inter}} = 0.07586$. The black lines of these four subfigures represent the critical curves for which $\Lambda = 0.0$, and the curves to the left and right denote the regions for $\Lambda > 0.0$ and $\Lambda < 0.0$, respectively, and indicate that the analytical derive condition is agrees well with the numerical results. So from these scenarios, one can conclude that for lower coupling strength ϵ_1 for tier-1, the $(p_{\text{inter}}, \epsilon_2)$ parameter space exhibits a mixed type of transition and such a mixed type of transition gradually decreases for higher values of ϵ_1. However, for sufficient larger values of ϵ_1, the critical threshold for ILS state is quite independent of ϵ_2. The coupling strength in tier-1 through the x variable plays an important role when the coupling strength ϵ_2 in tier-2 is large.

As the rewiring probabilities p_{inter} and p_r yield to change the intralayer and interlayer connectivities matrices $\mathscr{A}^{[\alpha]}(t)$ and $b(t)$ in Eq. (13), so the transverse Lyapunov exponent Λ also varies accordingly. Analytically, these probabilities do not appear explicitly in the transverse error dynamics, but numerically we have observed their dependency in Figs. 5 and 6. The ILS state only can emerge after a certain threshold of p_{inter}. Therefore, we can say that the stability analysis is valid for any rewiring probabilities. Although for the Rössler oscillator as individual dynamics, p_r (intralayer rewiring probability) yields a tiny enhancement tendency, but it may have more clear dependency by considering different oscillators.

V. GLOBAL STABILITY OF ILS STATE

Now we investigate the global stability condition of the ILS state. This guarantees the global convergence to a common trajectory of each replica node irrespective of initial conditions. To derive the global stability condition of the ILS state, we need the following assumptions on the dynamics of each isolate node, related to intralayer and interlayer coupling functions and topologies of the intralayer connections.

Assumption 1. The function F is a Lipschitz function, so there exists a positive constant M such that

$$\|F(\mathbf{x}) - F(\mathbf{y})\| \leqslant M\|\mathbf{x} - \mathbf{y}\|, \tag{17}$$

where $\|\cdot\|$ is the Euclidean norm.

This particular assumption is needed to derive the global stability conditions, which ensures the upper bound of the rate of change of the isolate dynamics in the phase space.

Assumption 2. The intralayer coupling function G_α is linear. Thus, we may consider that $G_\alpha(\mathbf{x}_i, \mathbf{x}_j) = G_\alpha(\mathbf{x}_i - \mathbf{x}_j)$, where G_α is the inner coupling matrix. Moreover, we assume that G_α is a symmetric positive semidefinite matrix.

The above assumption ensures us that all the eigenvalues of G_α are non-negative.

Assumption 3. The interlayer coupling function H is also linear and it is of the form $H(\mathbf{x}_i, \mathbf{y}_i) = H(\mathbf{x}_i - \mathbf{y}_i)$, where the interlayer inner-coupling matrix H is symmetric positive definite.

Therefore, all the eigenvalues of H are positive.

Assumption 4. The intralayer Laplacian matrix $\mathscr{L}^{[\alpha]}(t)$ corresponding to the tier α $(1 \leqslant \alpha \leqslant M)$ is symmetric for all $t \in \mathbb{R}^+$.

This assumption assures us that all eigenvalues of $\mathscr{L}^{[\alpha]}(t)$ are real for each time instance t. Moreover, it is a positive semidefinite matrix with one zero eigenvalue.

By considering the invariant conditions for ILS state and above assumptions, the equation of motion of the stochastic

multilayer hypernetwork becomes

$$\dot{\mathbf{x}}_i = F(\mathbf{x}_i) + \sum_{\alpha=1}^{M} \epsilon_\alpha \sum_{j=1}^{N} \mathscr{A}_{ij}^{[\alpha]}(t) G_\alpha(\mathbf{x}_j - \mathbf{x}_i) + \eta\, b_i^{[1]}(t) H(\mathbf{y}_i - \mathbf{x}_i),$$
$$\dot{\mathbf{y}}_i = F(\mathbf{y}_i) + \sum_{\alpha=1}^{M} \epsilon_\alpha \sum_{j=1}^{N} \mathscr{A}_{ij}^{[\alpha]}(t) G_\alpha(\mathbf{y}_j - \mathbf{y}_i) + \eta\, b_i^{[2]}(t) H(\mathbf{x}_i - \mathbf{y}_i). \tag{18}$$

As the interlayer coupling term vanishes after achieving the interlayer synchronization, the interlayer connections may be considered as unidirectional, i.e., $b^{[1]}(t) \neq b^{[2]}(t)$.

Consider the ILS error term for each replica as $\mathbf{e}_i = \mathbf{x}_i - \mathbf{y}_i$ for $i = 1, 2, \ldots, N$. Then, the rate of change of this error system can be written as

$$\dot{\mathbf{e}}_i = [F(\mathbf{x}_i) - F(\mathbf{y}_i)] - \sum_{\alpha=1}^{M} \epsilon_\alpha \sum_{j=1}^{N} \mathscr{L}_{ij}^{[\alpha]}(t) G_\alpha \mathbf{e}_j - \eta\big[b_i^{[1]}(t) + b_i^{[2]}(t)\big] H \mathbf{e}_i. \tag{19}$$

If we consider $\mathbf{e}$ as the stack of the error terms $\mathbf{e}_1, \mathbf{e}_2, \ldots, \mathbf{e}_N$, then in vectorial form, the above error equation can be written as

$$\dot{\mathbf{e}} = \bigoplus_{i=1}^{N} [F(\mathbf{x}_i) - F(\mathbf{y}_i)] - \sum_{\alpha=1}^{M} \epsilon_\alpha \mathscr{L}^{[\alpha]}(t) \otimes G_\alpha \mathbf{e} - \eta B(t) \otimes H \mathbf{e}, \tag{20}$$

where $\bigoplus$ and $\otimes$, respectively, denote the matrix direct sum and Kronecker product, $B(t) = \mathrm{diag}[b_1^{[1]}(t) + b_1^{[2]}(t), b_2^{[1]}(t) + b_2^{[2]}(t), \ldots, b_N^{[1]}(t) + b_N^{[2]}(t)]$, while $\mathbf{x}_i$ and $\mathbf{y}_i$ satisfy Eq. (18). It is clear that the intralayer and interlayer connections of the above error equation are time varying. So, in the context of global stability, the handling with these time-varying connections are quite difficult. Next, we transform the error system [Eq. (19)] to an appropriate time-average system where the time-varying interlayer connections are transformed to time-average connections, but we leave the intralayer connections as time varying.

To achieve the time-average reduction, we recall the following lemma which has been proved in Ref. [61].

Lemma 1. Suppose there exists a constant T (however large) for which the matrix-valued function $\Gamma(t)$ is such that

$$\frac{1}{T}\int_t^{t+T} \Gamma(\tau) d\tau = \bar{\Gamma} \tag{21}$$

for all t, and

$$\dot{\mathbf{x}}(t) = [A(t) + \bar{\Gamma}]\mathbf{x}(t), \quad \mathbf{x}(t_0) = \mathbf{x}_0, \quad t \geqslant t_0, \tag{22}$$

is uniformly exponentially stable. Then for sufficient fast switching

$$\dot{\mathbf{z}}(t) = [A(t) + \Gamma(t)]\mathbf{z}(t), \quad \mathbf{z}(t_0) = \mathbf{z}_0, \quad t \geqslant t_0, \tag{23}$$

is also uniformly exponentially stable.

This lemma describes that for sufficient fast switching, a time-varying system can be approximated by the corresponding time-average system.

Our time-varying interlayer connections are encoded by the two arrays, $b^{[1]}(t), b^{[2]}(t) \in \mathbb{R}^N$, where $b_i^{[l]}(t) = 1$ with probability p_{inter} and 0 with probability $1 - p_{\mathrm{inter}}$ for $i = 1, 2, \ldots, N$ and $l = 1, 2$.

Now we show that, for all $p_{\mathrm{inter}} \in (0, 1)$, the interlayer connections are fast switching; more precisely, the time-varying diagonal matrix $B(t)$ changes rapidly. Its ith diagonal element $b_i^{[1]}(t) + b_i^{[2]}(t)$ can take three possible values as follows:

$$b_i^{[1]}(t) + b_i^{[2]}(t) = 2 \text{ with probability } p_{\mathrm{inter}}^2,$$
$$= 1 \text{ with probability } 2p_{\mathrm{inter}}(1 - p_{\mathrm{inter}}),$$
$$= 0 \text{ with probability } (1 - p_{\mathrm{inter}})^2.$$

More elaborately, $b_i^{[1]}(t) + b_i^{[2]}(t)$ takes the value two if bidirectional interlayer connections are present. Its value is 1 if among them exactly one is present (i.e., for unidirectional interlayer coupling) and zero if none of them is present (i.e., the ith interlayer connection is not present).

Now to prove $B(t)$ is fast switching, it is sufficient to show that the N-tuple

$$\big[b_1^{[1]}(t) + b_1^{[2]}(t), b_2^{[1]}(t) + b_2^{[2]}(t), \cdots, b_N^{[1]}(t) + b_N^{[2]}(t)\big] \tag{24}$$

has very less probability to persist in the next time iteration.

If in the tuple [Eq. (24)] the numbers 2, 1, and 0 are respectively n_1, n_2, and $N - n_1 - n_2$, then the probability of persistence of the same tuple in next time instant is

$$2^{n_2}(p_{\mathrm{inter}})^{2n_1+n_2}(1 - p_{\mathrm{inter}})^{2N-2n_1-n_2}. \tag{25}$$

If N is large, then the above expression [Eq. (25)] is near zero as $p_{\mathrm{inter}} \in (0, 1)$. With this, we achieve our requirement that $B(t)$ is fast switching and changes very rapidly for any value of $p_{\mathrm{inter}} \in (0, 1)$.

Now, for sufficient long time T, we have

$$\frac{1}{T}\int_t^{t+T} b_i^{[l]}(\tau) d\tau = p_{\mathrm{inter}}, \quad i = 1, 2, \ldots, N \text{ and } l = 1, 2. \tag{26}$$

The above equation immediately yields

$$\frac{1}{T}\int_t^{t+T} B(\tau) d\tau = 2p_{\mathrm{inter}} I_N, \tag{27}$$

where I_N is the identity matrix of order N.

Then, using Lemma 1, the corresponding time-average system of the time-varying error system [Eq. (20)] can be written as

$$\dot{\mathbf{e}} = \bigoplus_{i=1}^{N} [F(\mathbf{x}_i) - F(\mathbf{y}_i)] - \sum_{\alpha=1}^{M} \epsilon_\alpha \mathscr{L}^{[\alpha]}(t) \otimes G_\alpha \mathbf{e} - 2\eta p_{\mathrm{inter}} I_N \otimes H \mathbf{e}, \tag{28}$$

where we consider $\Gamma(t) = -\eta B(t) \otimes H$, and

$$A(t) = \bigoplus_{i=1}^{N} [F(\mathbf{x}_i) - F(\mathbf{y}_i)] - \sum_{\alpha=1}^{M} \epsilon_\alpha \mathscr{L}^{[\alpha]}(t) \otimes G_\alpha.$$

Therefore, we can conclude that if the time-average error system [Eq. (28)] is uniformly exponentially stable, then the original error system [Eq. (20)] is also uniformly exponentially stable. Hence, we analyze the global stability of the ILS state in terms of global asymptotic stability of the time-average system [Eq. (28)].

But it is to be noted that this time-average approximation is irrespective of the interlayer probability p_{inter}, as for all values of p_{inter}, the interlayer connections are fast switching. Although the intralayer Laplacian matrices are time varying, they are independent of the intralayer rewiring probability.

Now we directly derive the global stability condition of the above error system [Eq. (28)]. The following proposition will be helpful in this purpose.

Proposition 1. If A is a real symmetric matrix of order N, then for all $\mathbf{x} \in \mathbb{R}^N$,

$$\lambda_{\min}[A]\mathbf{x}^{\text{tr}}\mathbf{x} \leqslant \mathbf{x}^{\text{tr}}A\mathbf{x} \leqslant \lambda_{\max}[A]\mathbf{x}^{\text{tr}}\mathbf{x},$$

where $\lambda_{\min}[A]$ and $\lambda_{\max}[A]$ are respectively the minimum and the maximum eigenvalues of A.

This proposition actually gives the bound of the quadratic form $\mathbf{x}^{\text{tr}}A\mathbf{x}$, where $\mathbf{x}^{\text{tr}}$ denotes the transpose of $\mathbf{x}$.

The global stability condition will be derived in terms of the convergence properties of the trajectory of each node in one layer associated to the trajectory of its counterpart node in another layer. Therefore, we define a Lyapunov function in terms of the error quantities as

$$V(t) = \frac{1}{2}\sum_{i=1}^{N}\mathbf{e}_i^{\text{tr}}\mathbf{e}_i. \tag{29}$$

The time derivative of the above Lyapunov function along the interlayer synchronization solution can be written as

$$\dot{V}(t) = \sum_{i=1}^{N}\mathbf{e}_i^{\text{tr}}\dot{\mathbf{e}}_i. \tag{30}$$

With the help of Eq. (28), the expression of $\dot{V}(t)$ becomes

$$\begin{aligned}\dot{V}(t) = &\sum_{i=1}^{N}(\mathbf{x}_i-\mathbf{y}_i)^{\text{tr}}[F(\mathbf{x}_i)-F(\mathbf{y}_i)]\\ &-\sum_{\alpha=1}^{M}\epsilon_\alpha\sum_{i=1}^{N}(\mathbf{x}_i-\mathbf{y}_i)^{\text{tr}}\sum_{j=1}^{N}\mathscr{L}_{ij}^{[\alpha]}(t)G_\alpha(\mathbf{x}_j-\mathbf{y}_j)\\ &-2\eta\sum_{i=1}^{N}(\mathbf{x}_i-\mathbf{y}_i)^{\text{tr}}p_{\text{inter}}H(\mathbf{x}_i-\mathbf{y}_i).\end{aligned} \tag{31}$$

The Cauchy-Schwarz inequality yields for all $\mathbf{x}, \mathbf{y} \in \mathbb{R}^d$

$$[\mathbf{x}-\mathbf{y}]^{\text{tr}}[F(\mathbf{x})-F(\mathbf{y})] \leqslant \|\mathbf{x}-\mathbf{y}\|\|F(\mathbf{x})-F(\mathbf{y})\|. \tag{32}$$

Again by the hypothesis F is Lipschitz, the above inequality is equivalent to

$$[\mathbf{x}-\mathbf{y}]^{\text{tr}}[F(\mathbf{x})-F(\mathbf{y})] \leqslant M[\mathbf{x}-\mathbf{y}]^{\text{tr}}[\mathbf{x}-\mathbf{y}]. \tag{33}$$

Using this result, the inequality (31) becomes

$$\begin{aligned}\dot{V}(t) \leqslant &\sum_{i=1}^{N}(\mathbf{x}_i-\mathbf{y}_i)^{\text{tr}}M(\mathbf{x}_i-\mathbf{y}_i)\\ &-\sum_{\alpha=1}^{M}\epsilon_\alpha\sum_{i=1}^{N}(\mathbf{x}_i-\mathbf{y}_i)^{\text{tr}}\sum_{j=1}^{N}\mathscr{L}_{ij}^{[\alpha]}(t)G_\alpha(\mathbf{x}_j-\mathbf{y}_j)\\ &-2\eta\sum_{i=1}^{N}(\mathbf{x}_i-\mathbf{y}_i)^{\text{tr}}p_{\text{inter}}H(\mathbf{x}_i-\mathbf{y}_i).\end{aligned} \tag{34}$$

In vectorial form, the above inequality can be written as

$$\begin{aligned}\dot{V}(t) \leqslant &M\mathbf{e}^{\text{tr}}\mathbf{e}-\sum_{\alpha=1}^{M}\epsilon_\alpha\mathbf{e}^{\text{tr}}[\mathscr{L}^{[\alpha]}(t)\otimes G_\alpha]\mathbf{e}\\ &-2\eta p_{\text{inter}}\mathbf{e}^{\text{tr}}[I_N\otimes H]\mathbf{e}.\end{aligned} \tag{35}$$

By Assumptions 2 and 4, we can conclude that $[\mathscr{L}^{[\alpha]}(t)\otimes G_\alpha]$ is a real symmetric matrix. The smallest eigenvalue of $\mathscr{L}^{[\alpha]}(t)$ is zero for all time t, and G_α is positive semidefinite. Therefore, the smallest eigenvalue of $[\mathscr{L}^{[\alpha]}(t)\otimes G_\alpha]$ is also zero. Also by Assumption 3, the smallest eigenvalue of $[I_N\otimes H]$ is $\lambda_{\min}[H]$. Now using proposition 1, the inequality (35) can be written as

$$\dot{V}(t) \leqslant [M-2\eta p_{\text{inter}}\lambda_{\min}[H]]\mathbf{e}^{\text{tr}}\mathbf{e}. \tag{36}$$

Since $p_{\text{inter}} > 0$ and $\lambda_{\min}[H] > 0$, the required global stability condition becomes

$$\eta > \frac{M}{2p_{\text{inter}}\lambda_{\min}[H]}. \tag{37}$$

The above condition ensures the convergence of each replica node to its counterpart node irrespective of their initial conditions. It depicts that, for global stability of the ILS state, the interlayer coupling strength η is inversely proportional to the interlayer rewiring probability p_{inter}.

If the interlayer inner coupling is vector coupling, then $H = \text{diag}(1, 1, 1)$, and therefore $\lambda_{\min}[H] = 1$. The Lipschitz constant M of the Rössler oscillator with the chosen system parameter is approximately 22.2. In this case, the required global stability condition reduces as $\eta > \frac{11.1}{p_{\text{inter}}}$.

VI. EXISTENCE OF INTRALAYER SYNCHRONIZATION STATE

In this manuscript, our main focus is to study the ILS state for the stochastic multilayer hypernetwork. By considering the invariant conditions [Eq. (8)] of the ILS solution, the equation of motion of the multilayer hypernetwork becomes

$$\begin{aligned}\dot{\mathbf{x}}_i = &F(\mathbf{x}_i)+\sum_{\alpha=1}^{M}\epsilon_\alpha\sum_{j=1}^{N}\mathscr{A}_{ij}^{[\alpha]}(t)G_\alpha(\mathbf{x}_i,\mathbf{x}_j)\\ &+\eta\, b_i^{[1]}(t)H(\mathbf{x}_i,\mathbf{y}_i),\\ \dot{\mathbf{y}}_i = &F(\mathbf{y}_i)+\sum_{\alpha=1}^{M}\epsilon_\alpha\sum_{j=1}^{N}\mathscr{A}_{ij}^{[\alpha]}(t)G_\alpha(\mathbf{y}_i,\mathbf{y}_j)\\ &+\eta\, b_i^{[2]}(t)H(\mathbf{y}_i,\mathbf{x}_i),\end{aligned} \tag{38}$$

where $b_i^{[1]}(t) = b_i^{[2]}(t)$ or $H(\mathbf{x}, \mathbf{x}) = 0$. Here each node in one layer is connected to its counterpart node in the other layer stochastically with probability $p_{\text{inter}} \in (0, 1)$. These interlayer connections are encoded by the two arrays $b_i^{[1]}(t)$ and $b_i^{[2]}(t)$. In this section, we investigate whether intralayer synchronization is possible in this network.

Intralayer synchronization is a phenomenon of a multiplex network where complete synchrony is observed between the nodes in each layer. In other words, in a particular layer, the trajectories of all the nodes converge to each other. Mathematically, there will exist two trajectories $\mathbf{x}_0(t), \mathbf{y}_0(t) \in \mathbb{R}^d$ corresponding to two layers such that $\|\mathbf{x}_i(t) - \mathbf{x}_0(t)\| \to 0$ and $\|\mathbf{y}_i(t) - \mathbf{y}_0(t)\| \to 0$ as $t \to \infty$.

This intralayer synchronization solution will be an invariant solution if and only if all the nodes in layer-1 (layer-2) coincide with $\mathbf{x}_0(t)$ [$\mathbf{y}_0(t)$] at some time $t = t_0$. Then at that time instant, the rate of changes of all the state variables in layer-1 and layer-2 should be identical. Thus for any two arbitrary distinct nodes k and l in layer-1, we have $\dot{\mathbf{x}}_k = \dot{\mathbf{x}}_l$. This immediately gives

$$\sum_{\alpha=1}^{M} \epsilon_\alpha \sum_{j=1}^{N} \left[\mathscr{A}_{lj}^{[\alpha]}(t) - \mathscr{A}_{kj}^{[\alpha]}(t)\right] G_\alpha(\mathbf{x}_0, \mathbf{x}_0) + \eta\left[b_l^{[1]}(t) - b_k^{[1]}(t)\right] H(\mathbf{x}_0, \mathbf{y}_0) = 0. \tag{39}$$

Similarly, the arbitrary two distinct nodes k and l in layer-2 yields

$$\sum_{\alpha=1}^{M} \epsilon_\alpha \sum_{j=1}^{N} \left[\mathscr{A}_{lj}^{[\alpha]}(t) - \mathscr{A}_{kj}^{[\alpha]}(t)\right] G_\alpha(\mathbf{y}_0, \mathbf{y}_0) + \eta\left[b_l^{[2]}(t) - b_k^{[2]}(t)\right] H(\mathbf{y}_0, \mathbf{x}_0) = 0. \tag{40}$$

Therefore, to maintain the identical rate of change in each individual layer, we must have

$$\sum_{j=1}^{N} \mathscr{A}_{lj}^{[\alpha]}(t) = \sum_{j=1}^{N} \mathscr{A}_{kj}^{[\alpha]}(t), \quad \text{or} \quad G_\alpha(\mathbf{x}_0, \mathbf{x}_0) = 0, \tag{41a}$$

$$b_l^{[1]}(t) = b_k^{[1]}(t), \quad \text{or} \quad H(\mathbf{x}_0, \mathbf{y}_0) = 0, \tag{41b}$$

$$b_l^{[2]}(t) = b_k^{[2]}(t), \quad \text{or} \quad H(\mathbf{y}_0, \mathbf{x}_0) = 0, \tag{41c}$$

for all $t \in \mathbb{R}^+$, $\alpha = 1, 2, \ldots, M$, and $\mathbf{x} \in \mathbb{R}^d$. Thus, the above three conditions are the invariant conditions for the intralayer synchronization state. The condition (41a) indicates that the intralayer in-degree of each node is equal or the intralayer coupling function G_α should vanish after achieving the intralayer synchronization state. While the condition (41b) restricts the interlayer degree of each node in layer-1 is constant or the interlayer coupling function H vanishes after achieving the intralayer synchronization state. Similarly, condition (41c) restricts interlayer connections and the coupling function for layer-2.

But the nontrivial intralayer synchronization state with chaotic individual dynamics generally comprises the complete synchronization solutions $(\mathbf{x}_0(t), \mathbf{y}_0(t))$ of two layers which are evolved independently. In other words, they may not be related by the interlayer coupling function H. Thus, $H(\mathbf{x}_0, \mathbf{y}_0) = 0$ and $H(\mathbf{y}_0, \mathbf{x}_0) = 0$ both are absurd.

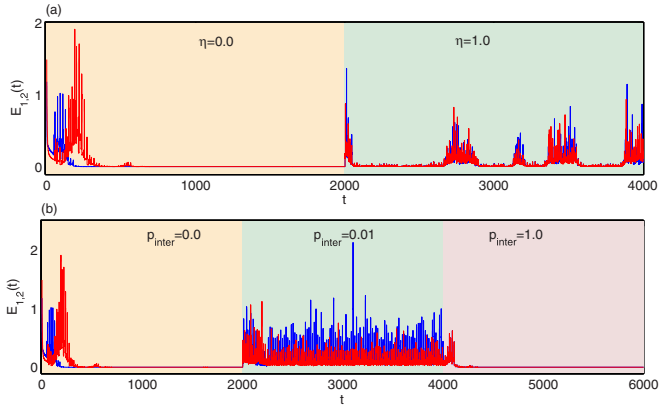

FIG. 7. Time evolution of the intralayer synchronization errors for layer-1 ($E_1(t)$, blue curve) and layer-2 ($E_2(t)$, red curve), respectively, at (a) $p_{\text{inter}} = 0.05$ and (b) $\eta = 1.0$. Other parameters values: $r_p = 10^{-6}$, $p_{\text{sw}} = 0.1$, $k = 2$, and $p_{\text{rand}} = 0.015$. Here, $E_1(t)$ and $E_2(t)$ are the respective instantaneous errors for layer-1 and layer-2 at time t.

Again, for our network model, we consider stochastic interlayer connections. Therefore, the interlayer may not present for some nodes in some time instant, i.e., $b_l^{[1]}(t)$ may not be equal to $b_k^{[1]}(t)$ at some time t. A similar thing can happen for the second layer also. Therefore, intralayer synchronization is impossible for a stochastic multiplex network, although it is possible for a blinking type of network [48], where all the replicas are either active or inactive for each time. For trivial intralayer synchronization (i.e., global synchronization) for which $\mathbf{x}_0(t) = \mathbf{y}_0(t)$ for all t, then $H(\mathbf{x}_0(t), \mathbf{y}_0(t))$ can be zero for diffusive-like coupling.

We also verify the above analytical assertion numerically. For this purpose, let us define the complete synchronization errors E_1 and E_2 for the respective layer-1 and layer-2 as

$$E_1 = \lim_{T\to\infty} \int_0^T \sum_{j=2}^{N} \frac{\|\mathbf{x}_j(t) - \mathbf{x}_1(t)\|}{T(N-1)} dt$$

and

$$E_2 = \lim_{T\to\infty} \int_0^T \sum_{j=2}^{N} \frac{\|\mathbf{y}_j(t) - \mathbf{y}_1(t)\|}{T(N-1)} dt.$$

As the intralayer synchronization in the whole multiplex network emerges due to the simultaneous occurrence of complete synchrony in both layers [60], so we define the intralayer synchronization in the form of

$$E_{\text{intra}} = \frac{E_1 + E_2}{2}.$$

Figure 7 depicts the numerical validation of the above invariant conditions for the intralayer synchronization state. The blue and red curves denote the complete synchronization error of layer-1 and layer-2, respectively. As long as the two layers are uncoupled (i.e., $\eta = 0.0$), the intralayer synchronization solution decays toward zero [denoted by the yellow region in Fig. 7(a)]. When the stochastic interlayer connections are switched on, i.e., $p_{\text{inter}} = 0.05$, for certain interlayer coupling strength $\eta = 1.0$ at time $t = 2000$, $E_1(t)$ and $E_2(t)$

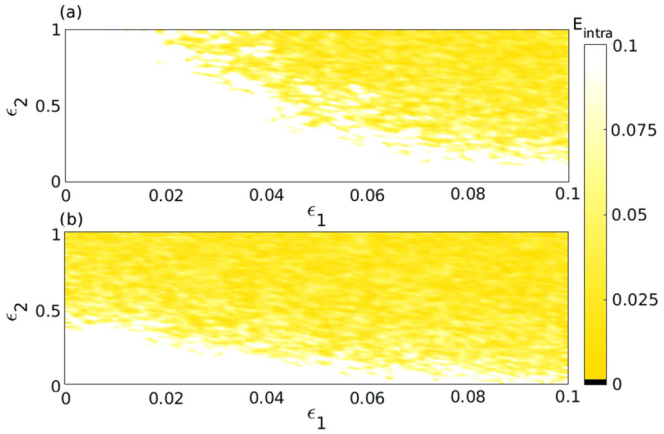

FIG. 8. Variation of the intralayer synchronization error E_{intra} in the (ϵ_1, ϵ_2) parameter plane for (a) $p_r = 10^{-6}$ and (b) $p_r = 10^{-2}$. Other parameter values are chosen as $p_{\text{inter}} = 0.05$, $p_{\text{sw}} = 0.1$, $k = 2$, and $p_{\text{rand}} = 0.015$. The black portion in the color bar represents $E_{\text{intra}} = 0.0$. Since in these parameter spaces, no black region appears, so intralayer synchronization does not emerge in the considered network.

immediately turn out to be nonzero (shown in the light cyan region) due to the violation of conditions (41b) and (41c). In Fig. 7(b), variations of $E_1(t)$ and $E_2(t)$ are plotted for $\eta = 1.0$ with three structurally different values of p_{inter} represented by three different colored regions. Initially from $t = 0$, p_{inter} is set as 0.0, i.e., both the layers are uncoupled. Then $E_1(t)$ and $E_2(t)$ asymptotically converge to zero. At time 2000, the value of p_{inter} is set as 0.01, and immediately $E_1(t)$ and $E_2(t)$ become nonzero and oscillate chaotically. From this time instance, the interlayer connections are stochastically rewired and violate the conditions (41b) and (41c). Again, at time $t = 4000$, the value of p_{inter} is set as 1, which gives a complete multiplex hypernetwork architecture and satisfies the invariance conditions (41b) and (41c). Then the intralayer synchronization errors $E_{1,2}(t)$ again asymptotically die out. From the above results, one can conclude that the intralayer synchronization solution becomes noninvariance in this network architecture due to the stochastic interlayer connections.

Further, the variation of E_{intra} is delineated in the (ϵ_1, ϵ_2) parameter plane in Fig. 8 for two different values of p_r, as in Fig. 2 [(a) $p_r = 10^{-6}$ and (b) $p_r = 10^{-2}$]. Here, it is clearly seen that in our network architecture the intralayer synchronization does not emerge. This verifies our analytical treatment regarding the invariance of intralayer synchronization. So the intralayer synchronization is not achievable in our considered stochastic multiplex hypernetwork.

VII. CONCLUSION

We have theoretically and numerically investigated the interlayer synchronization transition scenarios in general stochastic duplex hypernetworks. In this work, we derived the invariant conditions for the existence of ILS states in terms of intralayer Laplacian matrices and the nature of interlayer connections. Moreover, to analyze the stability of this synchronization state, we extend the master stability function framework to this certain class of multiplex networks. Hence, we analytically derived the necessary condition for the existence of the ILS state. Our local stability analysis for the ILS state does not require any conditions in terms of the Laplacian matrices and coupling functions, and hence this result can be applied to any network topologies and coupling functions. With few assumptions on isolate node dynamics, and intra- and interlayer coupling functions, we derive the global stability condition of the ILS state in a time-varying multilayer hypernetwork. We also investigated the existence condition for intralayer synchronization state and numerically we proved that the intralayer synchrony does not emerge due to the stochastic interlayer connections.

For numerical illustration, we consider a two-layer network of Rössler oscillators, where each layer consists of two different types of coupling configurations corresponding to two different tiers. Tier-1 is represented by the coupling through the x variable and its underlying network topology is an ER random network, whereas, in tier-2, the coupling happens through the y variable and its underlying network topology is an SW network. Each network of these two tiers is allowed to switch probabilistically. Also, each replica in this multiplex network is stochastically connected with a certain probability. Significantly for lower values of intralayer coupling strengths, we observed a tiny enhancement of the interlayer synchrony in intralayer-interlayer rewiring probability, and interestingly this enhancement no longer persists for higher values of intralayer coupling strength. We found mixed transition scenarios in the plane of interlayer probability and the strength of tier-2 in the absence of tier-1, but introducing tier-1 and gradually increasing its strength, the mixed region gradually shrinks and finally vanishes. We also notice that intralayer strength and intralayer network architecture are unfavorable for the emergence of interlayer synchrony. For other individual node dynamics and coupling configurations, the invariance and stability condition will be maintained, but the parameter space may vary.

Finally, we wish to point out that our study on interlayer coherence in a stochastic multiplex hypernetwork is more general and this analytical concept may be helpful to estimate the layer-layer coherence of any types of temporal multilayered architecture including biological networks to several types of engineered systems. Also, some real-world complex networks are associated with dynamical processes [14,64] and have multiplex organization [14,29], and in that case, such investigations may provide a proper tool to articulate the functional relations among each interacting individual unit.

ACKNOWLEDGMENTS

The authors acknowledge the anonymous referees for their insightful suggestions and comments. D.G. was supported by SERB-DST (Department of Science and Technology), Government of India (Project No. EMR/2016/001039).

APPENDIX

1. Global synchronization

Here we provide the proof of the global synchrony relation: Global synchrony emerges in a multilayer network if and only if intralayer and interlayer synchrony both occur

simultaneously and irrespective of individual nodal dynamics and coupling configurations. We assume that $\{\mathbf{x}_1(t), \mathbf{x}_2(t), \ldots, \mathbf{x}_N(t)\}$ and $\{\mathbf{y}_1(t), \mathbf{y}_2(t), \ldots, \mathbf{y}_N(t)\}$ are the state vectors of the two layers. If the underlying dynamical multilayer network is in ILS state, then we have

$$\mathbf{x}_i(t) = \mathbf{y}_i(t) \quad \text{for all} \quad i \in \{1, 2, \ldots, N\}. \tag{A1}$$

Again, due to its intralayer synchronization state, there exist intralayer synchronization $(\mathbf{x}_0(t), \mathbf{y}_0(t))$ such that

$$\mathbf{x}_i(t) = \mathbf{x}_0(t) \text{ and } \mathbf{y}_i(t) = \mathbf{y}_0(t) \quad \text{for all } i \in \{1, 2, \ldots, N\}. \tag{A2}$$

From Eqs. (A1) and (A2), we have $\mathbf{x}_0(t) = \mathbf{y}_0(t)$. Therefore $\mathbf{x}_i(t) = \mathbf{x}_0(t)$ and $\mathbf{y}_i(t) = \mathbf{x}_0(t)$ for all i. Thus $\mathbf{x}_0(t)$ is the global synchronization state variable of the multilayer network.

2. Unidirectional interlayer connections: Analytical stability condition

In this subsection, we derive the local stability condition for ILS in Eq. (11) with unidirectional interlayer connections. By considering the invariant conditions (8a) and (8b), Eq. (38) becomes the evolution equation of the multilayer hypernetwork with unidirectional interlayer connections where $H(\mathbf{x}, \mathbf{x}) = 0$ and $b^{[1]}(t) \neq b^{[2]}$.

For this type of multilayer hypernetwork, the ILS manifold is dominated by the equation of motion,

$$\dot{\mathbf{x}}_i = F(\mathbf{x}_i) + \sum_{\alpha=1}^{M} \epsilon_\alpha \sum_{j=1}^{N} \mathscr{A}_{ij}^{[\alpha]}(t) G_\alpha(\mathbf{x}_i, \mathbf{x}_j), \tag{A3}$$

$i = 1, 2, \ldots, N$. At ILS state, the ith node $(\mathbf{x}_i, \mathbf{y}_i)$ of both the layers evolve synchronously. Now consider small perturbation $\delta\mathbf{z}_i(t)$ of the ith node of layer-2 from the ILS state $\mathbf{x}_i = \mathbf{y}_i$. Then we have $\mathbf{y}_i = \mathbf{x}_i + \delta\mathbf{z}_i$, and the dynamics of $\delta\mathbf{z}_i$ can be written as

$$\begin{aligned}\delta\dot{\mathbf{z}}_i = &\left[DF(\mathbf{x}_i) + \eta\left\{b_i^{[2]}(t) JH(\mathbf{x}_i, \mathbf{x}_i) - b_i^{[1]}(t) DH(\mathbf{x}_i, \mathbf{x}_i)\right\}\right]\delta\mathbf{z}_i \\ &+ \sum_{\alpha=1}^{M} \epsilon_\alpha \sum_{j=1}^{N} \mathscr{A}_{ij}^{[\alpha]}(t)[JG_\alpha(\mathbf{x}_i, \mathbf{x}_j)\delta\mathbf{z}_i + DG_\alpha(\mathbf{x}_i, \mathbf{x}_j)\delta\mathbf{z}_j].\end{aligned} \tag{A4}$$

Here $\mathbf{x}_i$ is the dynamics of the ILS state satisfying Eq. (A3). Equation (A4) is the required master stability equation transverse to the ILS state for unidirectional interlayer connections.

[1] S. Boccaletti, V. Latora, Y. Moreno, M. Chavez, and D.-U. Hwang, Phys. Rep. **424**, 175 (2006).

[2] A. Pikovsky, J. Kurths, and M. Rosenblum, *Synchronization: A Universal Concept in Nonlinear Sciences* (Cambridge University Press, Cambridge, 2003).

[3] F. Sorrentino, New J. Phys. **14**, 033035 (2012).

[4] S. Rakshit, B. K. Bera, D. Ghosh, and S. Sinha, Phys. Rev. E **97**, 052304 (2018).

[5] A. E. Pereda, Nat. Rev. **15**, 250 (2014).

[6] B. L. Partridge and T. J. Pitcher, J. Comput. Physiol. **135**, 315 (1980).

[7] N. Abaid and M. Porfiri, J. R. Soc. Interface **7**, 1441 (2010).

[8] C. Zhou, L. Zemanova, G. Zamora, C. C. Hilgetag, and J. Kurths, Phys. Rev. Lett. **97**, 238103 (2006); New J. Phys. **9**, 178 (2007).

[9] S. V. Buldyrev, R. Parshani, G. Paul, H. E. Stanley, and S. Havlin, Nature **464**, 1025 (2010).

[10] M. Kurant and P. Thiran, Phys. Rev. Lett. **96**, 138701 (2006).

[11] S. Boccaletti, G. Bianconi, R. Criado, C. I. del Genio, J. Gómez-Gardeñes, M. Romance, I. Sendiña-Nadal, Z. Wang, and M. Zanin, Phys. Rep. **544**, 1 (2014).

[12] Mikko Kivelä, A. Arenas, M. Barthelemy, J. P. Gleeson, Y. Moreno, and M. A. Porter, J. Complex Netw. **2**, 203 (2014).

[13] G. Bianconi, *Multilayer Networks: Structure and Function* (Oxford University Press, Oxford, 2018).

[14] S. Pilosof, M. A. Porter, M. Pascual, and S. Kéfi, Nat. Ecol. Evol. **1**, 0101 (2017).

[15] M. Szell, R. Lambiotte, and S. Thurner, Proc. Natl. Acad. Sci. USA **107**, 13636 (2010).

[16] A. Cardillo, J. Gómez-Gardeñes, M. Zanin, M. Romance, D. Papo, F. del Pozo, and S. Boccaletti, Sci. Rep. **3**, 1344 (2013); A. Halu, S. Mukherjee, and G. Bianconi, Phys. Rev. E **89**, 012806 (2014).

[17] A. Cardillo, M. Zanin, J. Gómez-Gardeñes, M. Romance, A. García del Amo, and S. Boccaletti, Eur. Phys. J. Spec. Top. **215** (**1**), 23 (2013).

[18] B. Bentley, R. Branicky, C. L. Barnes, Y. L. Chew, E. Yemini, E. T. Bullmore, P. E. Vértes, and W. R. Schafer, PLoS Comput. Biol. **12**, e1005283 (2016).

[19] G. Blewitt, in *GPS for Geodesy*, edited by P. Teunissen and A. Kleusberg (Springer, Berlin, 1998), pp. 231–270.

[20] F. Radicchi and A. Arenas, Nat. Phys. **9**, 717 (2013).

[21] J. Gómez-Gardeñes, M. De Domenico, G. Gutiérrez, A. Arenas, and S. Gómez, Philos. Trans. A Math. Phys. Eng. Sci. **373**, 20150117 (2015).

[22] J. Gao, S. V. Buldyrev, H. E. Stanley, and S. Havlin, Nat. Phys. **8**, 40 (2012).

[23] G. Bianconi and S. N. Dorogovtsev, Phys. Rev. E **89**, 062814 (2014).

[24] A. Saumell-Mendiola, M. Á. Serrano, and M. Boguñá, Phys. Rev. E **86**, 026106 (2012).

[25] C. Granell, S. Gómez, and A. Arenas, Phys. Rev. Lett. **111**, 128701 (2013).

[26] C. Buono, L. G. Alvarez-Zuzek, P. A. Macri, and L. A. Braunstein, PLoS ONE **9**, e92200 (2014).

[27] J. Sanz, C.-Y. Xia, S. Meloni, and Y. Moreno, Phys. Rev. X **4**, 041005 (2014).

[28] G. Menichetti, L. Dall'Asta, and G. Bianconi, Sci. Rep. **6**, 20706 (2016).

[29] S. Gómez, A. Díaz-Guilera, J. Gómez-Gardeñes, C. J. Pérez-Vicente, Y. Moreno, and A. Arenas, Phys. Rev. Lett. **110**, 028701 (2013).

[30] R. G. Morris and M. Barthelemy, Phys. Rev. Lett. **109**, 128703 (2012).

[31] Z. Wang, A. Szolnoki, and M. Perc, J. Theor. Biol. **349**, 50 (2014).

[32] L. V. Gambuzza, M. Frasca, and J. Gómez-Gardeñes, Europhys. Lett. **110**, 20010 (2015).
[33] R. Sevilla-Escoboza, I. Sendiña-Nadal, I. Leyva, R. Gutiérrez, J. M. Buldú, and S. Boccaletti, Chaos **26**, 065304 (2016).
[34] I. Leyva, R. Sevilla-Escoboza, I. Sendiña-Nadal, R. Gutiérrez, J. M. Buldú, and S. Boccaletti, Sci. Rep. **7**, 45475 (2017).
[35] S. Rakshit, S. Majhi, B. K. Bera, S. Sinha, and D. Ghosh, Phys. Rev. E **96**, 062308 (2017).
[36] S. Rakshit, B. K. Bera, and D. Ghosh, Phys. Rev. E **98**, 032305 (2018).
[37] X. Zhang, S. Boccaletti, S. Guan, and Z. Liu, Phys. Rev. Lett. **114**, 038701 (2015).
[38] S. Jalan and A. Singh, Europhys. Lett. **113**, 30002 (2016).
[39] P. Holme and J. Saramäki, Phys. Rep. **519**, 97 (2012).
[40] S. Wasserman and K. Faust, *Social Network Analysis: Methods and Applications* (Cambridge University Press, Cambridge, 1994).
[41] J. P. Onnela, J. Saramaki, J. Hyvonen, G. Szabo, D. Lazer, K. Kaski, J. Kertesz, and A. L. Barabasi, Proc. Natl. Acad. Sci. USA **104**, 7332 (2007); Y. Wu, C. Zhou, J. Xiao, J. Kurths, and H. J. Schellnhuber, *ibid.* **107**, 18803 (2010); J. L. Iribarren and E. Moro, Phys. Rev. Lett. **103**, 038702 (2009).
[42] V. Kohar and S. Sinha, Chaos Solitons Fract **54**, 127 (2013).
[43] M. L. Sachtjen, B. A. Carreras, and V. E. Lynch, Phys. Rev. E **61**, 4877 (2000).
[44] D. Tanaka, Phys. Rev. Lett. **99**, 134103 (2007).
[45] R. Olfati-Saber, J. A. Fax, and R. M. Murray, Proc. IEEE **95**, 215 (2007).
[46] T. M. Przytycka, M. Singh, and D. K. Slonim, Brief Bioinform **11**, 15 (2010); S. Lèbre, J. Becq, F. Devaux, M. P. H. Stumpf, and G. Lelandais, BMC Syst. Biol. **4**, 130 (2010); A. Rao, A. O. Hero, D. J. States, and J. D. Engel, J. Bioinform. Sys. Biology **2007**, 51947 (2007).
[47] M. Valencia, J. Martinerie, S. Dupont, and M. Chavez, Phys. Rev. E **77**, 050905(R) (2008).
[48] I. V. Belykh, V. N. Belykh, and M. Hasler, Phys. D **195**, 188 (2004).
[49] V. Kohar, P. Ji, A. Choudhary, S. Sinha, and J. Kurths, Phys. Rev. E **90**, 022812 (2014).
[50] J. Lü and G. Chen, IEEE Trans. Autom. Control **50**, 841 (2005).
[51] M. Frasca, A. Buscarino, A. Rizzo, L. Fortuna, and S. Boccaletti, Phys. Rev. Lett. **100**, 044102 (2008); L. Prignano, O. Sagarra, and A. Díaz-Guilera, *ibid.* **110**, 114101 (2013).
[52] D. Levis, I. Pagonabarraga, and A. Díaz-Guilera, Phys. Rev. X **7**, 011028 (2017).
[53] S. Majhi, D. Ghosh, and J. Kurths, Phys. Rev. E **99**, 012308 (2019).
[54] L. M. Pecora and T. L. Carroll, Phys. Rev. Lett. **80**, 2109 (1998).
[55] P. Erdős and A. Rényi, Publ. Math. Debrecen **6**, 290 (1959).
[56] D. J. Watts and S. H. Strogatz, Nature **393**, 440 (1998).
[57] L. Tang, X. Wu, J. Lü, J.-a. Lu, and R. M. D'Souza, Phys. Rev. E **99**, 012304 (2019).
[58] R. Gutiérrez, I. Sendiña-Nadal, M. Zanin, D. Papo, and S. Boccaletti, Sci. Rep. **2**, 396 (2012).
[59] S. Majhi and D. Ghosh, Chaos **27**, 053115 (2017).
[60] S. Rakshit, B. K. Bera, J. Kurths, and D. Ghosh, Proc. R. Soc. A **475**, 20190460 (2019).
[61] D. J. Stilwell, E. M. Bollt, and D. G. Roberson, SIAM J. Appl. Dyn. Syst. **5**, 140 (2006).
[62] B. K. Bera, S. Rakshit, D. Ghosh, and J. Kurths, Chaos **29**, 053115 (2019).
[63] L. Huang, Q. Chen, Y. C. Lai, and L. M. Pecora, Phys. Rev. E **80**, 036204 (2009).
[64] U. Harush and B. Barzel, Nat. Commun. **8**, 2181 (2017).